CERTIFICATO DI FIRMA DIGITALE

Si certifica che questo documento informatico

phd_unisi_076750_1.pdf

composto da n°73pagine

È stato firmato digitalmente in data odierna con Firma Elettronica Qualificata (FEQ), avente l'efficacia e gli effetti giuridici equivalenti a quelli di una firma autografa, ai sensi dell'art. 2702 del Codice Civile e dell'art. 25 del Regolamento UE n. 910/2014 eIDAS (electronic IDentification Authentication and Signature).

PROCESSI INFORMATICI COMPLETATI

- **Apposizione di Firma Elettronica Qualificata Remota** emessa da Intesi Group S.p.A. in qualità di prestatore di servizi fiduciari qualificati autorizzato da AgID, per garantire con certezza l'autenticità, l'integrità, il non ripudio e l'immodificabilità del documento informatico e la sua riconducibilità in maniera manifesta e inequivoca all'autore, ai sensi dell'art. 20 comma 2 del CAD - D.lgs 82/2005.
- **Apposizione di Marca Temporale Qualificata** emessa da Intesi Group S.p.A. in qualità di prestatore di servizi fiduciari qualificati autorizzato da AgID, per attribuire una data e un orario opponibile a terzi, ai sensi dell'art. 20 comma 3 del CAD - D.lgs 82/2005 e per far sì che la Firma Elettronica Qualificata apposta su questo documento informatico, risulti comunque valida per i prossimi 20 anni a partire dalla data odierna, anche nel caso in cui il relativo certificato risultasse scaduto, sospeso o revocato.
- **Apposizione di Contrassegno Elettronico**, l'unica soluzione tecnologica che permette di prorogare la validità giuridica di un documento informatico sottoscritto con firma digitale e/o marcato temporalmente, rendendolo inalterabile, certo e non falsificabile, una volta stampato su supporto cartaceo, ai sensi dell'art. 23 del CAD - D.lgs 82/2005.

  Per risalire all'originale informatico è necessario scansionare il Contrassegno Elettronico, utilizzando l'applicazione HONOS, disponibile per dispositivi Android e iOS.

FIRMATO DIGITALMENTE DA:
Nome: NICLA
Cognome: LORITO
Data: 18 febbraio 2021

UNIVERSITÀ
DI SIENA
1240

Università degli Studi di Siena

Department of Biotechnology, Chemistry and Pharmacy

Research Doctorate in Biochemistry and Molecular Biology
BIBIM2.0

Cycle XXXIII°

Coordinator: Prof. Lorenza Trabalzini

Metabolic determinants of therapy resistance in estrogen receptor positive breast cancer

Scientific-disciplinary sector: BIO/10

PhD student: Nicla Lorito

Co-tutor: Dr. Andrea Morandi

Supervisor: Prof. Elisa Giannoni

Academic year 2019/2020

INDEX

Bacci, M.; **Lorito**, N.; Ippolito, L.; *et al*. Reprogramming of Amino Acid Transporters to Support Aspartate and Glutamate Dependency Sustains Endocrine Resistance in Breast Cancer. *Cell Rep.* **2019**

Lorito, N.; Bacci, M.; Smiriglia, A.; *et al*. Glucose Metabolic Reprogramming of ER+ Breast Cancer in Acquired Resistance to the CDK4/6 Inhibitor Palbociclib. *Cells*. **2020**

Bacci, M; **Lorito**, N.; *et al*. Fat and Furious: Lipid Metabolism in Anti-Tumoral Therapy Response and Resistance. *Trends in Cancer*. **2020**

Abbreviations

2-DG, 2-deoxyglucose
α-KG, alpha-ketoglutarate
acetyl-CoA, acetyl-coenzyme A
ACLY, ATP-citrate lyase
ADP, adenosine diphosphate
AI, aromatase inhibitors
ANOVA, analysis of variance
AP1, activator protein one
APC/C, anaphase promoting complex/cyclosome
ASL, argininosuccinate lyase
ASS, argininosuccinate synthetase
ATCC, American type culture collection
ATP, adenosine 5'-triphosphate
AURKA, aurora kinase A
BCA, bicinchoninic acid
BRCA, breast cancer gene
BSA, bovine serum albumin
CA IX, carbonic anhydrase nine
CAF, cancer associated fibroblasts
CBP, CREB binding protein
CCCA, complete cell cycle arrest
CDH1, cadherin one
CDK, cyclin-dependent kinases
CKI, CDK inhibitors
CQ, chloroquine
CSC, cancer stem cells
DABS, 4-N,N-dimethylaminoazobenzene-4'-sulfonyl chloride
DBD, DNA binding domain
DCA, dichloroacetate
DCC, dextran charcoal stripped FBS
DFS, disease free survival
DMEM, dulbecco's modified eagle medium
DMSO, dimethyl sulfoxide
E1, estrone
E2, 17-β-estradiol
E3, estriol
ECAR, extracellular acidification rate
ECM, extracellular matrix
EGFR, epidermal growth factor receptor
EMA, European Medicines Agency
EMT, epithelial-mesenchymal transition
ER, estrogen receptor
ERE, estrogen response elements
ET, endocrine therapy
ETC, electron transport chain
F26BP, fructose-2,6-bisphosphate
FASN, fatty acid synthase
FBP, fructose-1,6-bisphosphate
FBS, fetal bovine serum
FBXO4, F-box protein four
FCCP, carbonyl cyanide-4 (trifluoromethoxy) phenylhydrazone
FDA, Food and Drug Administration
FDG, ^{18}F-fluorodeoxyglucose
FDG-PET, fluorodeoxyglucose positron emission tomography
FGFR1, fibroblast growth factor receptor one
FH, fumarate hydratase
FOXM1, forkhead box M one

FSH, follicle stimulating hormone
FULVR, fulvestrant resistance
FZR1, fizzy-related protein homolog one
G6P, glucose-6-phosphate
GAPDH, glyceraldehyde-3-phosphate dehydrogenase
GC-MS, gas chromatography-mass spectrometry
GDH, glutamate dehydrogenase
GF, growth factor
GLS, glutaminase
GLUT, glucose transporters
glycoPER, glycolytic proton efflux rate
GnRH, gonadotropin-releasing hormone
GPx1, glutathione peroxidase one
GSA, glutamic-γ-semialdehyde
GSEA, gene set enrichment analysis
GSH, glutathione
HC, hydroxycholesterol
HCQ, hydroxychloroquine
HDAC, histone deacetylases
HER2, epidermal growth factor receptor two
HIF1-α, hypoxia-inducible factor one alpha
HK, hexokinase
HPLC, high-performance liquid chromatography
HRP, horseradish peroxidase
HRT, hormone replacement therapy
HSP, heat shock proteins
IC50, half maximal inhibitory concentration
IFN, interferon
IGF-1, insulin-like growth factor one
LBD, ligand binding domain
LC3, microtubule-associated protein 1A-1B-light chain three
LC-MS, liquid chromatography-mass spectrometry
LD, lipid droplets
LDH, lactate dehydrogenase
LH, luteinizing hormone
LTED, long-term estrogen deprived
MAPK, mitogen-activated protein kinase
MCT, mono-carboxylate transporters
MDM2, mouse double minute two homolog
MSTFA, N-trimethylsilyl-N-methyl trifluoroacetamide
mTOR, mammalian target of rapamycin
NADH, nicotinamide adenine dinucleotide
NADPH, nicotinamide adenine dinucleotide phosphate
NCOR, nuclear receptor corepressor
NF-κB, nuclear factor kappa-light-chain-enhancer of activated B cells
NO, nitric oxide
NR, nuclear receptor
Nrf2, nuclear factor erythroid related factor two
OCR, oxygen consumption rate
OS, overall survival
OXPHOS, oxidative phosphorylation
P5C, 1-pyrroline-5-carboxylate
PBS, phosphate buffered saline
PCA, principal component analysis
PD, palbociclib
PDH, pyruvate dehydrogenase
PDK1, 3-phosphoinositide-dependent protein kinase one
PDK1, pyruvate dehydrogenase kinase one
PDR, palbociclib resistance
PDX, patient-derived xenografts

PEP, phosphoenolpyruvate
PFK1, phosphofructokinase one
PFKFB3, 6-phosphofructo-2-kinase/fructose-2,6-biphosphatase three
PFS, progression free survival
PHGDH, 3-phosphoglycerate dehydrogenase
PIK3CA, phosphatidylinositol-4,5-bisphosphate 3-kinase alpha
PKB, protein kinase B
PKM2, pyruvate kinase M2
PPARγ, peroxisome proliferator-activated receptor gamma
PPP, pentose phosphate pathway
PR, progesterone receptor
PRODH, proline dehydrogenase
PTEN, phosphatase and tensin homolog
PYCR, P5C reductase
qRT-PCR, quantitative real-time polymerase chain reaction
Rb, retinoblastoma
RET, rearranged during transfection
RFS, relapse free survival
ROS, reactive oxygen species
RTK, tyrosine kinase receptor
SB, sample buffer
SDS-PAGE, sodium dodecyl sulphate-polyacrylamide gel electrophoresis
SERD, selective ER downregulators
SERM, selective ER modulators
SHMT, serine hydroxy-methyltransferase
SLC1A2, solute carrier family 1 member 2
SLC6A14, solute carrier family 6 member 14
SMAD3, mothers against decapentaplegic homolog three
SP1, specific protein one
SRC, steroid receptor coactivator
SREBP, sterol regulatory element-binding transcription factor
STAT3, signal transducer and activator of transcription three
TAMR, tamoxifen resistance
TCA, tricarboxylic acid
TCA, trichloroacetic acid
TGF-β, transforming growth factor beta
TNBC, triple negative breast cancer
TNFAIP3, tumor necrosis factor alpha-induced protein three
TNFR, tumor necrosis factor receptor
TRAF6, TNFR-associated factor six
UTP, uridine-5’-triphosphate
VEGF, vascular endothelial growth factor

Abstract

The majority of breast cancers are estrogen receptor positive (ER+) and epidermal growth factor receptor two negative (HER2-) and are dependent on estrogens for their growth and survival. Endocrine therapy (ET), which acts by targeting the ER signaling pathway, is the standard of care for these tumors. Unfortunately, ~40% of women relapse with ET resistant disease and understanding the metabolic reprogramming underlying such resistance is an important need. In the first part of this thesis, we performed a global gene expression analysis in ET resistant compared to parental cells revealing a downregulation of the neutral and basic amino acid transporter SLC6A14 governed by enhanced miR-23b-3p expression, resulting in impaired amino acid uptake. Biochemical and biological assays showed that this deregulation of the amino acid metabolism is supported by autophagy activation and increased import of acidic amino acids (i.e., aspartate and glutamate) mediated by the cognate SLC1A2 transporter in ET resistant cells. We then analyzed aspartate and glutamate destiny by radioactive tracing assay and LC-MS, and we observed that both amino acids (i) fuel lipid, protein, and nucleotide biosynthesis and (ii) enhance ^{13}C-labelled TCA cycle intermediates (e.g., citrate, α-ketoglutarate, succinate, fumarate, and malate) together with uridine-5'-triphosphate (UTP, DNA synthesis) and glutamine (protein synthesis) levels, indicating that both glutamate and aspartate boost TCA and interrelated anaplerotic pathways in ET resistant cells compared to the parental counterpart. Interestingly, Seahorse analysis showed that the concomitant deprivation of aspartate and glutamate in ET resistant cells significantly impaired oxygen consumption rate and subsequent oxidative potential, whereas the withdrawal of each single amino acid has no effect, suggesting that the mitochondrial-dependent catabolism is sustained by either one or the other amino acid. The clinical relevance of these findings is validated by multiple orthogonal approaches in large cohorts of ET treated patients and in patient-derived xenografts (PDX). Targeting amino acid metabolic reprogramming re-sensitizes ET resistant cells to the therapy and impairs their aggressive features (e.g., proliferation, invasion, clonogenicity/stemness), including their metastatic ability in *in vivo* experiments.

In the second part of the thesis, we decided to broaden the investigation of therapy resistance in ER+ breast cancer, based on the notion that, recent clinical trial have shown that a superior clinical outcome is achieved in a subset of ER+/HER2- metastatic breast cancer patients receiving a combination of a cyclin-dependent kinases 4 and 6 (CDK4/6) inhibitor (e.g., palbociclib, PD) together with the standard ET. Moreover, CDK4/6 inhibitors have also been tested in ER+/HER2+ preclinical breast cancer models and reported encouraging results. Despite the clinical advances of a combinatorial therapy using ET plus CDK4/6 inhibitors, potential limitations (i.e., PD resistance) could emerge and investigating the metabolic adaptations underlying such resistance warrants further elucidations. Thus, we subjected a panel of ER+ breast cancer cells sensitive to PD (PDS) and their resistant derivatives (PDR) to a metabolic profiling using an array of complementary high-end techniques including ^{14}C-radioactive glucose tracing, western blotting, and qRT-PCR analysis of key metabolic enzymes, together with Seahorse analysis coupled to gas chromatography-mass spectrometry (GC-MS). This approach revealed a differential metabolic behavior of PDR cells when compared to PDS, independently of their proliferative status. Moreover, the metabolic phenotype of the PDR cells showed significant differences between cells that are HER2+ and HER2-. Specifically, ER+/HER2+ PDR cells are characterized by enhanced glucose dependency in both basal and under metabolic stress conditions compared to PDS cells. Conversely, ER+/HER2- PDR cells exhibit a decreased glycolytic phenotype compared to their parental counterpart. We have therefore targeted these glucose dependencies using 2-deoxyglucose, glucose deprivation, galactose-containing medium, and HK2 (hexokinase two) silencing. Crucially, glycolysis inhibition re-sensitizes ER+/HER2+ PDR cells to PD as well as potentiates the response of ER+/HER2- PDS cells to the therapy. Finally, HK2 higher-expressing ER+/HER2+ breast cancers show a worse prognosis when compared to the lowering-expressing patients, even in multivariate analysis, suggesting that HK2 may characterize a subset of tumors more susceptible to therapy resistance and subsequent relapse.

In conclusion, our results suggest that the deregulated tumor metabolism could represent a strategic mechanism that sustains therapy resistance and offer a series of predictive biomarkers and potential targetable pathways to be exploited to combat or delay ET resistance in ER+ breast cancer.

Chapter I. Introduction

1. Breast cancer

Breast cancer is the second most frequently diagnosed cancer in the world and the leading cause of cancer-related death in women with almost 2 million cases and 600,000 deaths in 2018. Breast cancer incidence varies widely, ranging from less favorable trends in Northern America, Western Europe, and Australia (e.g., 92 per 100,000 in Northern America) to lowest rates in Africa, Southern Asia, and Central America (e.g., 27 per 100,000 in Middle Africa). In Italy, nearly 60,000 new cases have been diagnosed in 2019. In terms of mortality, the trend is opposite with lowest rates in high- and middle- income countries. This dichotomy is largely influenced by life expectancy, breast cancer screening campaigns, and better diagnostic technologies together with an array of therapeutic opportunities allowing early diagnosis and tailored treatment, thus resulting in improved prognosis of breast cancer patients [1, 2]. Breast cancer predisposition is influenced by reproductive-related factors such as advanced maternal age for the first pregnancy, early menarche, and late-onset menopause, together with modifiable risk factors including obesity, physical inactivity, and alcohol abuse, and also involves familiarity and genetic predisposition. About 10% of breast cancers are inherited and associated with a family history. Mutations in two high-penetrance tumor suppressor genes, *BRCA1* and *BRCA2* (breast cancer gene one and two), are associated with a 70% probability to develop breast cancer by the age of 80 years [3].

Adenocarcinoma is the most common type of breast cancer representing more than 95% of mammary tumors and arises from the glandular tissue. Depending on the site of origin, these cancers are classified as ductal and lobular carcinomas that originate from either the breast ducts or lobules, respectively. Both ductal and lobular carcinomas are defined *in situ* when confined within the primary site, and invasive when metastasize to adjacent and/or distal tissues. The majority of breast cancers are ductal carcinomas with only a 10% of invasive lobular carcinoma, that is the most frequent in women between 45 and 55 years old [4]. **Figure 1** provides additional information on these histological subtypes.

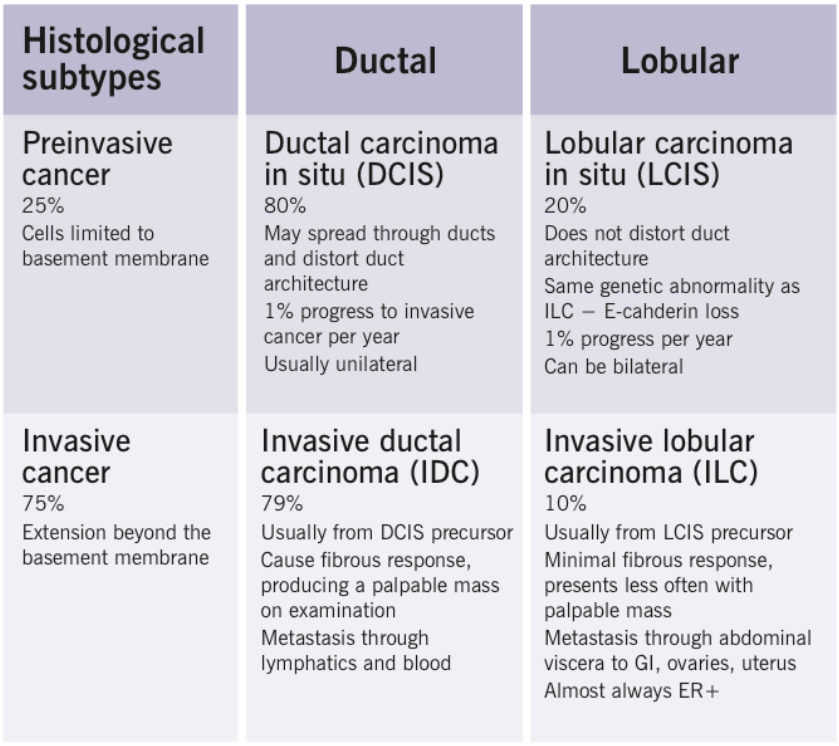

Figure 1. Histological subtypes of breast cancer (adapted from E. Wong (2012) Breast cancer pathogenesis and histologic vs. molecular subtypes. Pathophysiology Review).

From a clinical point of view, the current management of breast cancer comprises a selection of treatment modalities including surgery, chemotherapy (e.g., anthracyclines, taxanes), radiotherapy, hormonal therapy (endocrine therapy, ET), and targeted treatments (e.g., the antibody against the epidermal growth factor receptor two, HER2, trastuzumab). Most breast cancers are removed surgically by either local excision or mastectomy (i.e., complete removal of the breast). Patients can be treated with neo-adjuvant hormonal therapy or chemotherapy with the aim of reducing the tumor size prior to surgery. Following clinical excision, breast cancers are assessed for their size, grade, and the presence of local lymph vascular invasion together with the genetic and molecular profile, all information needed for cancer staging and subsequent therapeutic intervention.

1.1 Molecular subtypes of breast cancer

Breast cancer is a highly heterogeneous disorder with an extremely variable biological and clinical behavior, and understanding such histological and molecular vulnerability is crucial to determine the appropriate therapy. Over the last decades, genomic, transcriptomic, and proteomic analyses have been applied to identify innovative molecular markers with prognostic and/or predictive value. Initial studies of gene expression profile identified four major groups of breast cancer associated to specific phenotypic characters and clinical outcomes, according to the expression of a series of genes that could be reconducted to the presence of estrogen receptor (ER) and/or progesterone receptor (PR), and the overexpression of HER2. The main

molecular subsets classified are luminal-like, HER2+, basal-like, and normal-like. Additionally, the luminal subtype can be further categorized into three different subgroups, according to their distinct expression profiles: luminal A, that are mostly ER+, HER2-, and/or PR+, characterized by high expression of ER-related genes and low levels of the proliferation marker Ki-67; luminal B that are ER+ and/or PR+, can express HER2 and HER2-related genes and, in addition, express a consistent set of genes related to proliferation and cell cycle; and the new heterogeneous subtype luminal C showing a more aggressive progression than luminal A or B [5]. The biological behavior of these cancers is correlated with their gene expression profile: luminal A tumors are the most commonly diagnosed, typically low grade, and usually responsive to ET with a positive prognosis; in contrast, luminal B have a worse prognosis with reduced overall survival (OS) [5]. The HER2+ subset is characterized by the overexpression and/or amplification of HER2, that is a member of the EGFR (epidermal growth factor receptor) family with tyrosine kinase activity, and is usually ER- and PR-. The amplification or overexpression of HER2 approximately occurs in 15–30% of breast cancers. This kind of tumors have a significantly higher therapeutic response compared to HER2- cancers thanks to the introduction of the HER2-targeted therapy [6], while showing poorer prognosis than luminal subtypes. Basal-like cancers are characterized by the absence of ER, PR, and HER2 and the upregulation of genes expressed by basal/myoepithelial cells, and are more common in women with *BRCA1* mutations. These tumors are typically high grade and show poor response, thereby resulting in an early metastatic disease [7]. Finally, the normal-like subtype is ER+, PR+, and HER2-, has low levels of the protein Ki-67 and a slightly worse prognosis than luminal A tumors [5].

In summary, the classification into ER+, HER2+, and triple-negative (ER, PR and HER2-) breast cancer (TNBC) is clinically relevant, since the current management is centered on anti-estrogen treatment, HER2 targeted agents, and chemotherapy. These molecular subtypes have different prognostic index and clinical outcome, thus requiring distinct therapeutic regimes [8], described in **Figure 2**.

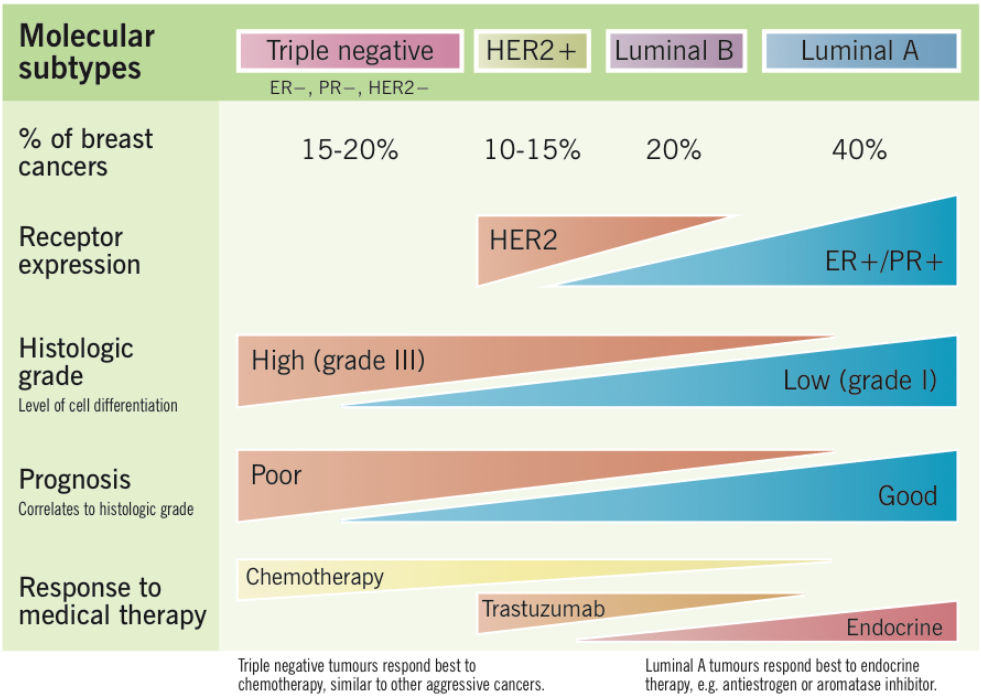

Figure 2. Molecular subtypes of breast cancer (adapted from E. Wong (2012) Breast cancer pathogenesis and histologic vs. molecular subtypes. Pathophysiology Review).

More recently, further studies of gene expression profiling identified additional and rare subtypes of breast cancer including the “claudin-low”. This subtype is characterized by the absence of hormonal receptors and HER2, low levels of proteins involved in the cell-cell adhesion known as claudins, and high expression of stem cell features, immune-related proteins (e.g., CD79b and CD14), and markers of migration and angiogenesis (e.g., integrin α5 and vascular endothelial growth factor A, VEGFA, respectively) [9].

1.2 Estrogen receptor positive breast cancer

Approximately 80% of breast cancers are positive for ER and/or PR and negative for HER2 [10]. In the normal human breast, 10-15% of mammary luminal epithelial cells express ER at detectable levels but do not proliferate, although they are in close proximity to proliferating cells. Interestingly, estrogen stimulation of ER+ breast cells induces the release of paracrine factors which in turn promote the proliferation of the surrounding ER- epithelial cells [11]. In contrast, ER+ human breast cancer cells promptly proliferate and, since they are dependent on estrogens for their growth and survival [10], inhibiting this dependency with the ET that targets ER pathway is the standard of care for this subset of tumors. ER+ breast cancers are well differentiated, less aggressive, and associated with better outcome after surgery when compared with ER- tumors [12]. Indeed, about two-third of ER+ breast cancers regress after estrogen deprivation mediated by hormonal therapy [13].

1.2.1 Estrogen and breast cancer risk

Estrogens belong to the steroid hormone class synthesized from cholesterol and mainly secreted by ovaries. The three main forms of estrogens are: estrone (E1), estradiol (E2, or 17β-estradiol), and estriol (E3). E2 is the major product derived from the biosynthetic process and the most potent estrogen in premenopausal women. Such female sexual hormones play a key role in the development and maintenance of the reproductive function and regulate physiological processes in the cardiovascular, skeletal, immune, and central nervous system [14]. Furthermore, estrogens are also involved in the development and progression of breast cancer. Estrogen physiological and pathological effects are generally mediated by ER, which acts as a transcription factor regulating the expression of ER-dependent genes [15].

Ovary and adipose tissue represent the principal source of estrogens, although the site of production differs between pre and postmenopausal women. In premenopause, estrogen synthesis predominantly occurs in the ovary under the control of the hypothalamic-pituitary-ovarian axis. Indeed, the ovarian production is stimulated by the hypothalamic gonadotropin-releasing hormone (GnRH) which, in turn, induces the pituitary release of luteinizing hormone (LH) and follicle stimulating hormone (FSH). LH stimulates androgen production by theca cells while FSH upregulates the aromatase enzyme which converts androgen into estrogen in the granulosa cells. Estrogens are then released into blood circulation and reach distal estrogen responsive tissues. Ovarian synthesis of estrogens stops at menopause when distal organs including adipose tissue, bone, vascular endothelium, aortic smooth muscle, and brain become the main source of production [16]. This localized and peripheral production plays an important role in tumor progression in postmenopausal women, in which the intratumoral concentration of E2 is more than 20-fold higher of that present in the plasma due to the conversion of androgens into estrogens that occurs in breast tumor and surrounding tissue [17].

Estrogens play a key role in the etiology of breast cancer thanks to their proliferative effect and the exposure to estrogens is associated with an increased risk of breast cancer [18]. The molecular mechanisms underlying this increased risk related to estrogen exposure are not fully elucidated. Factors associated with a higher incidence of breast cancer include early menarche, late menopause, late first full-term pregnancy, and the use of the hormone replacement therapy (HRT). Such strong association between estrogen and breast cancer risk may be explained by two hypotheses: (i) estrogen binding to ER promotes the transcription of genes involved in cell proliferation enhancing errors and mutations generated during DNA replication thus resulting in an altered cellular division which sustains the neoplastic transformation [19]; (ii) estrogens can be transformed into genotoxic compounds (e.g., quinone derivatives), which directly bind and damage DNA by acting as free radicals [20]. In addition, the prolonged exposure to other hormones involved in estrogen signaling, such as prolactin [21], progesterone [18], and testosterone [22], may also exert a role in increasing breast cancer risk.

1.2.2 Estrogen receptor and mechanism of action

Estrogen effects are mediated by two ERs, estrogen receptor α (ERα) and estrogen receptor β (ERβ), that belong to the nuclear receptor (NR) superfamily and act as transcription factors [23]. ERα is mainly expressed by gonadal organs and at low levels in bone, liver, kidney, and adipose tissue; in contrast, non-gonadal tissues such as colon, lung, and brain express ERβ. Co-expression of both receptors occurs in mammary glands, thyroid, epididymis, bone, and regions of the brain. ERα and ERβ are two distinct proteins of 595 and 530 amino acids respectively, encoded by distinct genes located on different chromosomes: *ESR1* on chromosome 6 and *ESR2* on chromosome 14, respectively [24].

Mechanistically, estrogens bind to ER and trigger a series of conformational changes allowing its transactivation consisting of receptor dimerization, as either homodimer (ERα/ERα or ERβ/ERβ) or heterodimer (ERα/ERβ), translocation to the nucleus, recruitment of and interaction with coactivators and other transcription factors. The dimeric receptor binds to small palindromic sequences known as estrogen response elements (ERE), located within the promoter of the target genes. This interaction and the subsequent recruitment of coactivators induce the transcription of ER-dependent genes. In particular, the p300/CREB binding protein (CBP) coactivator synergistically cooperates with ER to increase the efficacy of the ligand-dependent transcriptional activation [25, 26].

ERs are structurally related and evolutionarily conserved and contain several structural domains, defined by the putative functions enclosed in each region (**Figure 3**). The highly conserved DNA binding domain (DBD, region C) contains two zinc finger motifs and is involved in DNA binding and receptor dimerization, whereas the ligand binding domain (LBD, region E) mediates the estrogen binding and the subsequent receptor dimerization, nuclear translocation, and interaction with transcriptional coactivators and corepressors. Region F contains a ligand activable transcriptional domain AF-2, whereas the N-terminal A/B region contains a ligand-independent domain AF-1 that regulates the transcription in response to phosphorylation events orchestrated by growth factor (GF) signaling, including MAPK (mitogen-activated protein kinase) and AKT or PKB (protein kinase B) pathways. Finally, the hinge domain (D-H) includes the nuclear localization signal of the receptor and provides the flexibility of the two moieties containing DNA and ligand binding sites [27-29].

ERα and ERβ show a sequence homology of >95% in DBD, 60% in LBD, and <25% in the N-terminal domain (**Figure 3**), thereby explaining the different response of the two receptors [30, 31]. They have similar affinity for estrogen and bind to the same DNA response elements. However, the biological role of ERβ is still controversial and knockout experiments in mice revealed a new unique role for ERβ. Indeed, while ERα induces the transcription of pro-proliferative and anti-apoptotic genes thus promoting cell proliferation and leading to carcinogenesis and tumor progression, ERβ stimulates the transcription of anti-proliferative and

pro-apoptotic genes, potentially playing a protective role against breast cancer [32, 33]. Here I will limit my discussion to ERα, hereafter called ER.

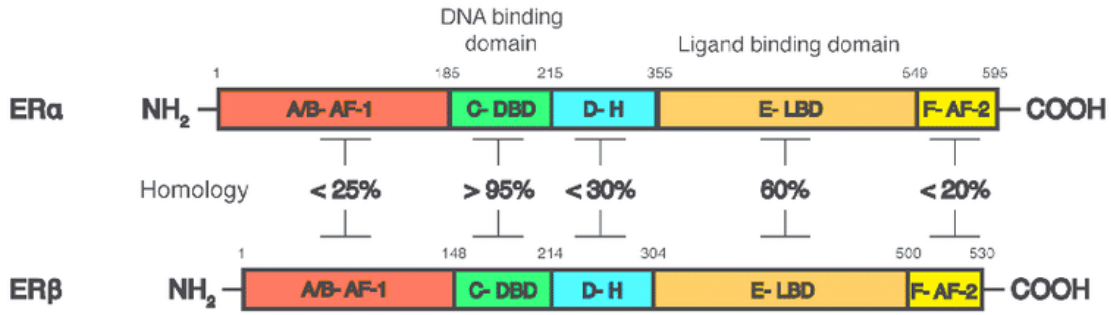

Figure 3. Schematic representation of the structural and functional domains of human ERα and ERβ (adapted from [34]).

The ligand-dependent ER mechanism of action can be classified into genomic and non-genomic signaling (**Figure 4**). The genomic pathway is the classical mechanism in which estrogens bind to the cytoplasmic ER and induce a conformational modification of the receptor causing its dissociation from the HSP (heat shock proteins), which typically maintain ER in the inactive form, and the consequent receptor dimerization and activation. The estrogen-ER complex translocates into the nucleus where binds to ERE thus promoting the transcription of ER-dependent genes. The indirect genomic signaling (known as tethered signaling) also exists and provides the interaction between estrogen activated ER and transcription factors, thus affecting gene transcription in the absence of a direct binding to the DNA. Indeed, several genes do not contain ERE in the promoter region but can be regulated by estrogen thanks to the interaction between ER and transcription factors such as AP1 (activator protein 1), SP1 (specific protein 1), and NF-κB (nuclear factor kappa-light-chain-enhancer of activated B cells). Conversely, the non-genomic pathway consists in the estrogen binding to a plasma membrane form of ER which activates a signaling cascade via second messengers also leading to a physiological response [28, 35]. Finally, as mentioned above, ER can be activated by ligand-independent mechanisms mediated by GF receptors. Indeed, the GF binding to the cognate receptor can activate downstream signaling events promoting the phosphorylation of the AF-1 domain hence activating ER in absence of the ligand and promoting the transcription of ER-dependent genes through the recruitment of different transcriptional coregulators [28].

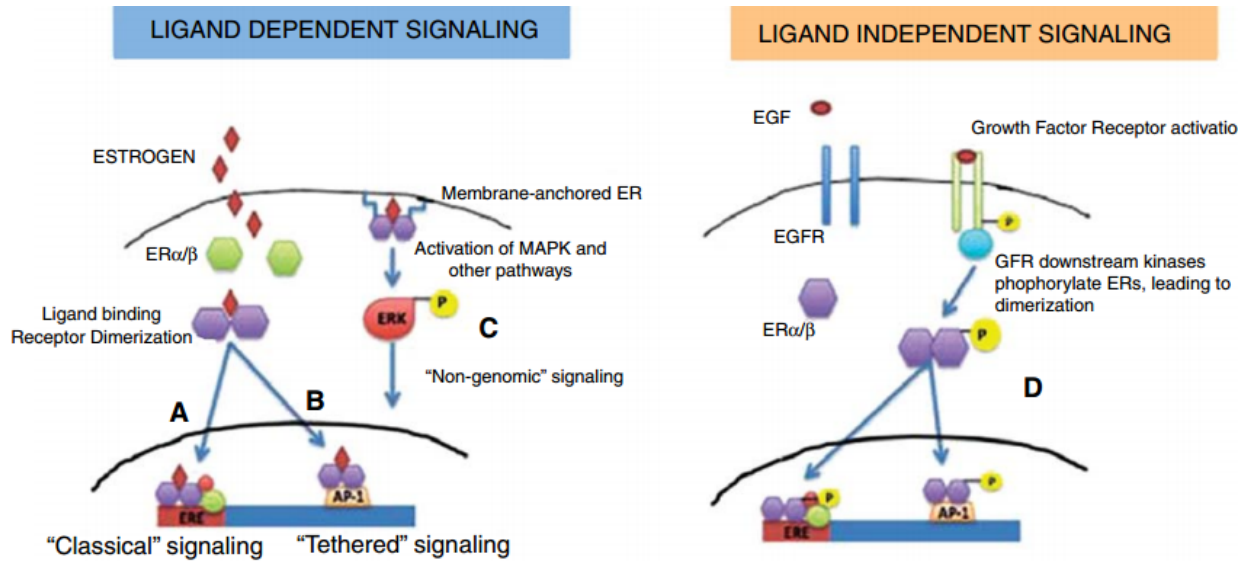

Figure 4. Schematic illustration of the key ER signaling pathways.

Among these, SRC (steroid receptor coactivator) proteins interact with the AF-2 domain and exert acetyltransferase activity mediating the transcriptional activation by the direct histone acetylation (i.e., major transcription activity). The p300/CBP complex further modifies chromatin through histone acetylation and/or methylation to enhance the ER-mediated transcription [15]. ER action is also regulated by several factors that act as corepressors. The nuclear receptor corepressor one (NCOR1) and two (NCOR2) interact with ER in absence of the ligand and induce the recruitment of histone deacetylases (HDAC), thus suppressing the transcription [36].

Many of the ER-dependent genes are involved in cell proliferation, apoptosis, angiogenesis, invasion, and metastasis formation. For example, the nuclear transcription factor c-Myc promotes the cell cycle progression and exerts a central role also in protein biogenesis, cell adhesion, metabolism, and signal transduction thus representing a crucial oncogenic driver and an attractive therapeutic target. Indeed, c-Myc is often deregulated in cancer and it has been found overexpressed in 20-30% of breast cancers. Inhibition of c-Myc prevents cellular proliferation induced by estrogens [37]. *CCND1* is a further important ER target gene which encodes for the cyclin D1 protein. Cyclin D1 binds to and activates cyclin-dependent kinases (CDK) 4 and 6 promoting cell cycle progression through the phosphorylation (i.e., inactivation) of cell cycle inhibitory substrates, such as retinoblastoma (Rb) protein [38]. Numerous efforts have been made to impair cyclin D1 activity and one the most effective consists in targeting the cyclin D1-associated kinases [38, 39], as I will describe later. Another approach to treat cyclin D1-dependent cancers is based on the notion that *CCND1* expression is also mTOR (mammalian target of rapamycin)-dependent, suggesting that mTOR inhibitors might reduce cyclin D1 abundance and block cell cycle progression, more effectively in a combinatorial treatment with CDK4/6 inhibitors [40].

2. Cell cycle

Cell cycle is a complex series of events in which cellular components are synthesized, DNA is duplicated, and the replicated chromosomes are accurately separated into two daughter cells before cell division. The duration of the cell cycle changes among different human cells. A typical highly proliferating cell divides approximately every 24 hours. Other types, such as embryonic cells, can replicate more rapidly; in contrast, some adult cells may stop or divide occasionally just to replace cells lost due to damage or death. The correct progression of the cell cycle is regulated in a both spatial and temporal manner by a conserved regulatory system. This system consists of phases and checkpoints which are essential for pausing a cell cycle phase if the conditions are not suitable for the cell division (e.g., genetic damage or abnormal cell size) but also serves to translate in mitogenic signals the extracellular inputs that control cell proliferation [41].

2.1 Control of the cell cycle: phases and checkpoints

Cell cycle consists of two consecutive processes divided into four interrelated phases: interphase which includes G1 (gap 1), S (synthesis), and G2 (gap 2) phases, and M (mitosis) phase (**Figure 5**). The two gaps separate and coordinate phases S and M. Importantly, these phases are not periods of cell inactivity but serve to produce the biomass required for cell division. Specifically, G1 is the interval between a previous mitosis and the following DNA replication, in which the cell is metabolically working and constantly growing. In this phase, the cell prepares DNA synthesis, tightly controlled by the first checkpoint, and starts the transcription of cell cycle-related genes. DNA replication occurs in S phase and is followed by the G2 phase during which cell growth continues and a second check on size and DNA duplication errors occurs. During M phase consisting of prophase, metaphase, anaphase, and telophase, chromatin is condensed and chromosomes are segregated into two diploid cells. Alterations in M phase can have severe outcomes, leading to cell death or deregulated cell proliferation [42]. Cytokinesis is the last step of cell division and ends when the cytoplasm of a single cell is separated into two daughter cells that are genetically identical to the parental cell. After completing one cycle of division, the cell may either resume with G1 phase or stay quiescent into G0 phase. In the G0 phase, cells are metabolic active but do not grow unless appropriate extracellular GF stimuli appear [43].

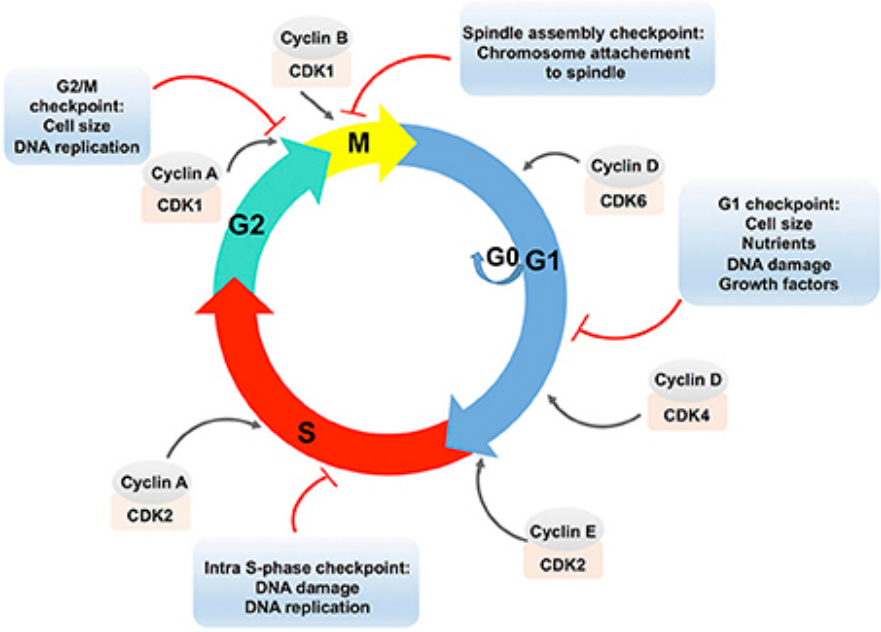

Figure 5. Schematic representation of cell cycle phases and checkpoints (taken from [44]).

Three main checkpoints closely regulate the different stages of the cell cycle and ensure that the complete genome is transmitted to daughter cells. Indeed, it is essential to prevent the cell entry into the next step of the cell cycle until the conclusion of the previous phase. Alternatively, daughter cells would fail to inherit the complete genetic material and undergo the so-called catastrophic cell division. The coordination of the various cell cycle phases is dependent on CDK and the timed-expression of their activating proteins known as cyclins [45] (**Figure 5**).

CDK are a family of serine/threonine kinases that are activated at specific points of the cell cycle and modulated by the interaction with cyclins and CDK inhibitors (CKI). Currently, more than 20 CDK have been identified [46] and five of them play a major role in the cell cycle progression (i.e., CDK4, CDK6, and CDK2 in phase G1, CDK2 during S phase, and CDK1 in mitosis), a process that could be altered in cancer [47, 48].

CDK expression remains stable during the cell cycle and their activation depends on the protein levels of their regulatory cyclins, that are synthesized and degraded by ubiquitin-mediated proteolysis in response to growth stimuli and, in this manner, they regularly activate CDK. Distinct cyclins are required according to the different phases of the cell cycle and act by controlling kinase activity and substrate specificity. Particularly, in response to mitogenic signals, three cyclin D (cyclin D1, D2, D3) types bind to and activate CDK4 and CDK6. The cyclin D-CDK4/6 complex is essential for the entry in G1 [49] and catalyzes the phosphorylation and subsequent inactivation of Rb, inducing the release of the transcription factor E2F and resulting in the induction of E2F responsive genes required for cell cycle progression [50]. Among these, *CCNE* encodes cyclin E which activates CDK2 by binding and completes the Rb phosphorylation further promoting the transcription of genes required for the entrance into S phase and the passage through the restriction checkpoint G1/S. CDK2 also plays an important

role in S phase progression by binding cyclin A. This complex phosphorylates proteins involved in DNA replication [51]. During G2/M checkpoint and mitosis, CDK1 binds first to cyclin A and then to cyclin B to regulate the transition from late G2 until the exit from mitosis [52]. Finally, an additional checkpoint controls the M phase and is the spindle checkpoint that prevents the transition to anaphase when the spindle fibers are not correctly connected to the chromosome kinetochores. In summary, each cyclin-CDK complex harbors unique functions limited to a specific phase of the cell cycle. Additional regulatory CDK cooperate for the correct cell cycle progression such as CDK7 which acts in combination with cyclin H as a CDK activating kinase [53].

Activity and function of the cyclin-CDK complexes are regulated by two families of CKI: the INK4 family (e.g., p16INK4a, p15INK4b) that specifically inactivates CDK4 and CDK6, and the Cip/Kip family (e.g., p21Cip1, p27Kip1) that inhibits cyclin E-, cyclin A-CDK2, as well as cyclin A-, cyclin B-CDK1 [54].

2.2 Role of the cyclin D1/cyclin-dependent kinases 4/6 complex in the cell cycle

CDK4/6 associate with and are activated by D-type cyclins to drive the transition from G1 to S phase of the cell cycle. The most important targets of this complex are the tumor suppressor Rb and the Rb-related proteins p107 and p130. In absence of GF stimuli, Rb couples with and inhibits the transcription factor E2F. CDK4/6-mediated Rb phosphorylation gradually induces the release of E2F, allowing the transcription of E2F target genes, and is a crucial step in driving the G1/S transition and ultimately promoting cell cycle progression [55] (**Figure 6**).

Unlike other cyclins that are regularly produced and degraded during the cell cycle, cyclin D is controlled by extracellular mitogenic signaling. In particular, it has been reported that ER can induce G1 phase progression and sustain cell proliferation by enhancing the expression of cyclin D1 encoded by *CCND1* that is one of the most important ER target genes [56] (**Figure 6**).

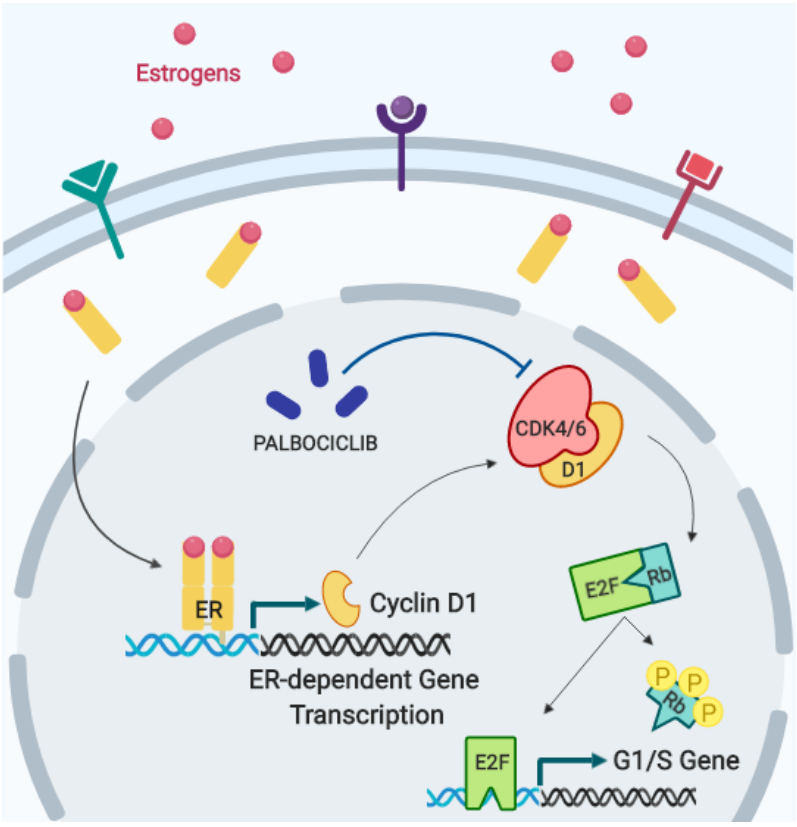

Figure 6. Mechanism of action of the cyclin D1-CDK4/6 complex.

Alterations such as cyclin D overexpression, CDK4/6 amplification, and loss of negative regulators potentiate the activity of the cyclin D-CDK4/6 complex which hyperphosphorylates Rb leading to uncontrolled cell proliferation. Thus, CDK4/6 targeting has emerged as a promising anti-cancer therapy [39].

Interestingly, cyclin D-CDK4/6 may drive proliferation and survival also through Rb-independent mechanisms. Indeed, CDK4/6 can phosphorylate other substrates such as the transcription factor FOXM1 (forkhead box M one) [57], the APC/C (anaphase promoting complex/cyclosome) activator CDH1 (cadherin one) [58], and a mediator of the TGF-β (transforming growth factor beta) anti-proliferative signaling, SMAD3 (mothers against decapentaplegic homolog three) [59], to drive cell cycle progression. In addition, cyclin D-CDK4/6 complex acts by removing the cell cycle inhibitors p21 and p27 from the complexes containing CDK2 [60].

CDK4/6 are more than mere regulators of the cell cycle. A growing body of literature shows that they are multifunctional proteins involved in cell cycle-independent processes. For example, the cyclin D3-CDK6 complex can phosphorylate and inactivate key glycolytic enzymes such as phosphofructokinase one (PFK1) and pyruvate kinase M2 (PKM2) fueling NADPH (nicotinamide adenine dinucleotide phosphate) and glutathione (GSH) production to reduce ROS (reactive oxygen species) accumulation and sustain cell survival [61].

3. Breast cancer therapy

Clinically, breast cancer is classified into three main classes categorized according to the expression of ER and PR and the overexpression/amplification of HER2. The three subtypes have different risk profiles and care strategies that include surgery, radiotherapy, chemotherapy, ET, and targeted therapy.

Eradicating tumor with surgery is the principal approach for treating early-stage and localized breast cancer and could be preceded by neo-adjuvant (pre-operative) therapy to reduce tumor mass. Moreover, surgery is usually followed by adjuvant (post-operative) therapy to guarantee the recovery and prevent or minimize the risk of metastatic recurrence. Specifically, cancer cells that survive surgical resection can be removed directly with high levels of radiation or chemotherapy. The choice of the systemic adjuvant therapy for not metastatic breast cancer should be determined by the intrinsic molecular phenotype: it is recommended ET for endocrine responsive tumor and HER2 targeted therapy for HER2+ tumor with some patients requiring also chemotherapy, while patients with TNBC receive chemotherapy. Otherwise, the therapeutic goal for women with inoperable metastatic breast cancer is to prolong life and symptom palliation using the same set of therapies [62, 63].

3.1 Endocrine therapy

ER+ breast cancer is the most prevalent subtype of mammary tumors and is dependent on estrogen for growth and survival. ET, that acts by interfering with ER signaling thus resulting in tumor growth inhibition, is the standard of care for this type of tumors. Currently, ET is the most effective therapy for ER+ breast cancer and exerts its inhibitory effect either by blocking estrogen action through a competitive antagonist of ER or by depriving tumor of estrogens [64].

Originally, endocrine ablation by ovariectomy in premenopausal women was used to prevent tumorigenesis and contrast tumor recurrence [65] and has now been replaced by three different classes of anti-hormonal agents, selective ER modulators (SERM), selective ER downregulators (SERD), and aromatase inhibitors (AI), together with drugs used to suppress estrogen production (e.g., goserelin that is a GnRH agonist).

SERM have been intensively studied over the past and have shown efficacy in treating different conditions related to postmenopause such as osteoporosis and ER+ breast cancer [66, 67]. They act by binding intracellular ER as a result of the structural similarity with estrogen and the mechanism of action depends on their tissue-selective ER agonist or antagonist activity [68]. The first developed SERM was MER25, a nonsteroidal anti-estrogen agent able to block estrogen action [69]. However, MER25 failed due to toxicity issues (e.g., hallucinations) and the first successful estrogen antagonist to enter the clinic was tamoxifen (ICI46,474) [70]. Although

SERM offer several therapeutic benefits, they also have some potentially serious adverse effects, such as thromboembolic disorders and uterine cancer.

SERD are a class of ER antagonists that induce ER downregulation by selectively degrading the receptor. Fulvestrant (Faslodex or ICI182,780) is a high affinity competitive antagonist of ER promoting its proteasome-dependent degradation [71] and is now considered to be a first-in-class SERD for patients with metastatic ER+ breast cancer [72]. Unfortunately, fulvestrant has substantial pharmaceutical limits (e.g., requiring intramuscular injection) which negatively impact on its extensive usage [73]. More recently, the development of orally bioavailable SERD, some of which have been clinically evaluated in clinical trials in breast cancer patients who have progressed on standard ET, may provide the possibility of blocking ER signaling in advanced metastatic breast cancer [74].

Finally, AI reduce estrogen levels by preventing their peripheral synthesis through the inhibition of the aromatase enzyme, which catalyzes the conversion of androgens into estrogens. Three generations of AI have been developed with the third generation showing a more favorable tolerability and selectivity profile compared to first- and second-generation agents. Currently, AI represent the gold standard for the treatment of early and advanced ER+ breast cancer in postmenopausal women [75, 76].

3.1.1 Tamoxifen

Tamoxifen belongs to SERM and is a pioneering drug for the treatment of ER+ breast cancer. In particular, it is the most commonly used endocrine agent as first-line adjuvant therapy in premenopausal women with ER+ tumors [70]. Structurally, tamoxifen is a nonsteroidal triphenylethylene derivative anti-estrogen that acts by competing with estrogen and binding ER, thus blocking the downstream molecular signaling and reducing breast cancer cell proliferation [77] (**Figure 7**).

The anti-cancer activity of tamoxifen occurs via its active metabolites, 4-hydroxy-tamoxifen and 4-hydroxy-N-desmethyltamoxifen. The affinity of 4-hydroxy-tamoxifen for ER is comparable to that of E2 [78]. More specifically, the anti-tumoral effect of tamoxifen is mediated not only by the competitive inhibition of ER but also by inducing an ER conformational change that prevents the binding of coactivators and induces the recruitment of transcriptional corepressors [79]. Consequently, the transcription of estrogen-dependent genes is blocked resulting in the cell cycle arrest in G1 phase. Furthermore, it has been shown that tamoxifen may also directly induce apoptosis through the production of ROS, changes in cell membrane fluidity, and induction of mitochondrial permeability [80]. The active metabolite 4-hydroxy-tamoxifen has been reported to induce the accumulation of autophagic vacuoles leading to apoptosis, suggesting a possible role for autophagy in the regulation of 4-hydroxy-tamoxifen-induced cell

death [81]. Additionally, tamoxifen has been described to have inhibitory effect on the mitochondrial respiratory capacity [82, 83].

Depending on the tissue, tamoxifen can act both as estrogen agonist and antagonist. In particular, it acts as an ER antagonist in breast, while it exerts agonistic effect in other sites such as vascular system and endometrium [84], where it has been reported that tamoxifen promotes the expression of ER target genes that do not contain a classical ERE, such as c-Myc and IGF1 (Insulin-like Growth Factor 1), both implicated in the regulation of cell proliferation, survival, and malignant transformation [85]. This agonistic activity is related to serious side effects such as thromboembolic events and uterine cancer [86, 87]. Whether tamoxifen acts as antagonist or agonist of the ER signaling depends on the cellular context. As discussed in paragraph 1.2.2, ER contains two domains that regulate the transcriptional activation, AF-1 and AF-2 (**Figure 3**). Since ER activity in breast is mainly driven by the ligand-dependent AF-2 domain, tamoxifen acts largely as an antagonist. Conversely, in other organs such as uterus, ER activity is also controlled by the ligand-independent AF-1 domain, resulting in greater agonistic tamoxifen activity [88].

Compelling data have demonstrated a significant OS benefit in ER+ breast cancer patients, with the tamoxifen treatment resulting in a 51% reduction in tumor recurrence and a 28% reduction in death as well as in improved life quality for patients with metastatic disease [89]. Tamoxifen has also been shown to be effective in reducing the incidence of breast cancer in patients at risk for developing the disease [90] and in women with ductal carcinoma *in situ* [91].

Despite these recognized benefits, not all patients with ER expressing tumors respond to this endocrine agent (*de novo* resistance) and a substantial group of responsive patients experience disease progression or recurrence (acquired resistance). Most patients with metastatic disease and 40% of early-stage breast cancer patients treated with adjuvant tamoxifen relapse with a tamoxifen resistant disease [92]. The biological mechanisms underlying resistance remain still unclear, but several hypotheses have been formulated, including the loss of ER expression and function, altered expression patterns of coregulatory proteins, the crosstalk between ER and GF receptors, and cell cycle checkpoint alterations [93].

3.1.2 Fulvestrant

Although adjuvant ET is an effective treatment for ER+ breast cancer, the majority of patients with an advanced disease will most likely exhibit resistance to the individual therapy [94]. Moreover, an initial response to the first endocrine treatment is generally indicative of a positive response to further alternative endocrine agents [95]. Consequently, the therapeutic options for ER+ breast cancer have been extended beyond SERM.

Fulvestrant represents a possible addition to the variety of endocrine treatments for postmenopausal women with advanced ER+ breast cancer and is the most commonly used

second-line agent after prior therapy with tamoxifen or AI [96, 97]. Fulvestrant belongs to the class of SERD and is a steroidal anti-estrogen compound that exerts its anti-tumoral role by preventing the estrogen-ER interaction, thus abrogating the estrogen-regulated transcriptional activity. Specifically, fulvestrant impairs the receptor dimerization and the energy-dependent nucleus-cytoplasm shuttling, thereby blocking the nuclear translocation of ER. Moreover, the ER-fulvestrant complex is instable and susceptible to a rapid proteasome-dependent degradation [98] (**Figure 7**).

In contrast to tamoxifen, which exclusively blocks the AF-2 domain and also exhibits partial agonistic activity, fulvestrant is considered a "pure" anti-estrogen that displays a higher ER affinity [99, 100] and induces a conformational change of ER resulting in the impairment of both AF-2 and AF-1 related transcriptional activities. Therefore, fulvestrant exhibits full ER antagonism and no agonistic effects [101].

Fulvestrant shows similar efficacy to tamoxifen as first-line therapy in patients with advanced ER+ breast cancer and to the AI anastrozole as second-line therapy in patients whose disease has progressed on prior ET [102]. Moreover, as monotherapy, fulvestrant may have superior efficacy than AI in patients who have not received adjuvant ET and in patients with inoperable locally or advanced breast cancer. However, despite clinical benefits, resistance to fulvestrant also frequently occurs [103]. Recent studies have shown numerous molecular mechanisms involved in fulvestrant resistance such as *PIK3CA* (phosphatidylinositol-4,5-bisphosphate 3-kinase α) and *ESR1* mutations [104]. The main side effects related to fulvestrant are nausea, asthenia, pain, vasodilatation, and headache [96].

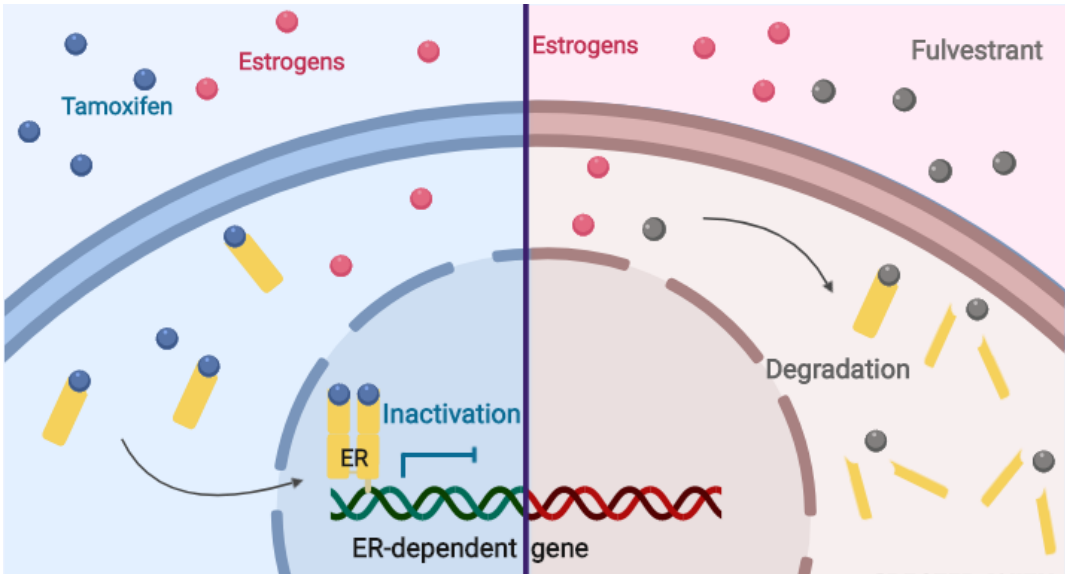

Figure 7. Tamoxifen and fulvestrant mechanism of action.

3.1.3 Aromatase inhibitors

AI administration is restricted to women without functional ovaries. Indeed, in premenopausal patients, AI ineffectively repress estrogen production [105] and should not be used alone. Conversely, in postmenopausal women, AI significantly decrease estrogen levels by blocking their peripheral synthesis. This is due to the fact that in premenopause the major estrogen source is the ovarian production, whereas after menopause estrogens derive exclusively from non-glandular tissues, in particular from the subcutaneous fat.

Aromatase is a member of the cytochrome P450 superfamily, encoded by *CYP19A1* gene located on the chromosome 15, and catalyzes the rate-limiting final step of the estrogen synthesis that is the conversion of androgenic precursors (i.e., androstenedione and testosterone) to estrogens (**Figure 8**). Aromatase expression is elevated in ovarian granulosa cells and depends on the cyclical gonadotropin stimulation. It is also present in several extra-gonadal tissues, including subcutaneous fat, liver, muscle, brain, bones, vascular endothelium, and normal breast adipose tissue [106]. Furthermore, it has been demonstrated that aromatase expression and activity are significantly increased in malignant compared to normal breast tissue, resulting in a higher intratumoral estrogen concentration [107, 108].

Blocking the conversion of androgen into estrogen, AI deprive tumor of estrogen thus reducing the ER signaling and causing a significant reduction of the estrogen-dependent proliferation in cancer cells [109] (**Figure 8**).

AI are classified into three generations according to their time of development and entry into the clinical setting, efficacy and mechanisms of action. The first- (e.g., aminoglutethimide) and second-generation AI (e.g., fadrozole and vorozole) were less selective and they also decreased aldosterone and cortisol production. The utility of these compounds was limited due to poor tolerability and adverse effects resulting in inadequate clinical efficacy [110]. Third generation AI are highly selective for the aromatase enzyme and well tolerated from patients showing only minor side effects. Two classes of third generation AI have been described: the nonsteroidal inhibitors (e.g., anastrozole and letrozole) that reversibly bind aromatase and the steroidal AI (e.g., exemestane) that irreversibly inhibit the enzyme [111].

Third generation orally available AI have now surpassed tamoxifen as first-line adjuvant therapy for postmenopausal women with metastatic ER+ breast cancer [112], showing significantly greater disease free survival (DFS), lower metastatic recurrence, and reduced incidence of contralateral breast cancer. Indeed, AI have no (partial) agonist activity thus reducing adverse effects as thromboembolic events, vaginal bleeding, and endometrial cancer [113]. However, despite clinical benefits, resistance emerges in approximately 50% of adjuvant treated patients and is inevitable in metastatic breast cancer [114].

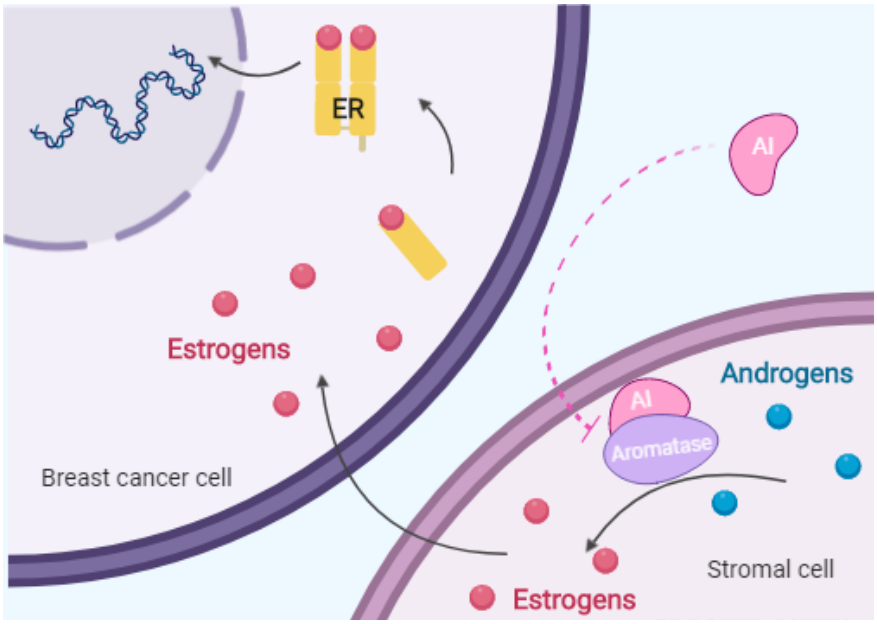

Figure 8. Aromatase inhibitor mechanism of action.

3.2 Cyclin-dependent kinases 4/6 inhibitors

Despite considerable advances in treating ER+ breast cancer patients with ET, resistance still remains the major cause of morbidity and mortality ultimately raising the need for new therapeutic approaches. The uncontrolled cell proliferation is an established hallmark of cancer [115] and the detailed understanding of cell cycle regulation and imbalance has contributed to the development of innovative and promising anti-cancer therapies. In particular, the dysregulation of the cyclin D1-CDK4/6-Rb axis signaling drives the phosphorylation of tumor suppressors and transcription factors ultimately contributing to a cell cycle unchecked progression [116]. In consideration of this pivotal role, extensive studies have been conducted to evaluate CDK4/6 as effective targets in cancer, especially in breast cancer.

The opening results with the first generation CDK inhibitors (e.g., flavopiridol, R-roscovitine, and UCN-01) were mostly disappointing due to their broad specificity in blocking a consistent number of CDK (pan-CDK inhibitors) and inadequate clinical activity observed *in vivo* resulting in poor efficacy, significant toxicity, and insuperable adverse effects [117]. Furthermore, the lack of applicable patient selection and the absence of predictive biomarkers may also have impacted on the initial failure. Flavopiridol is the most extensively investigated first generation CDK inhibitor that is not specific for a single CDK while acts as a pan-CDK inhibitor showing repressive effect on CDK1, CDK2, CDK4, CDK6, CDK7, and CDK9 [118, 119]. This compound not only exerts a cytostatic effect mediated by the cell cycle inhibition but also causes apoptosis, autophagy, transcriptional repression, and endoplasmic reticulum stress [120-122]. Phase I and II studies enrolling flavopiridol have shown low efficacy and off-target effects in healthy tissues providing severe toxicities typical of cytotoxic agents such as neutropenia, hyperglycemia, gastrointestinal, cardiac, and pulmonary disfunction [123, 124].

The second generation class showed superior specificity for preferential CDK with little or no suppression of other kinases and randomized clinical trials have validated that inhibitors highly selective for CDK4/6 are effective for the treatment of ER+/HER2- locally advanced or metastatic breast cancer in combination with ET [125]. The use of the CDK4/6 inhibitors has become common for this subset of patients and will certainly increase in the future.

Three CDK4/6 inhibitors, palbociclib (PD0332991, Ibrance, Pfizer), ribociclib (LEE011, Kisqali, Novartis), abemaciclib (LY2835219, Verzenio, Lilly), have received the approval by Food and Drug Administration (FDA) and European Medicines Agency (EMA) and are currently used in the clinical management of ER+/HER2- breast cancer patients. More specifically, palbociclib and ribociclib have a similar prescription. They are used as first-line therapy in postmenopausal patients with ER+/HER2- locally advanced or metastatic breast cancer in combination with an AI or in women previously treated with ET in combination with fulvestrant [FDA. Ibrance Prescribing Information. Available from: https://www.accessdata.fda.gov/drugsatfda_docs/label/2017/207103s004lbl.pdf; FDA. Kisqali Prescribing Information. Available from: https://www.accessdata.fda.gov/drugsatfda_docs/label/2017/209092s000lbl.pdf]. Abemaciclib is the only CDK4/6 inhibitor that can be administered as monotherapy in patients with ER+/HER2- metastatic breast cancer previously treated with ET and chemotherapy as well as in combination with fulvestrant as second-line therapy in women with ER+/HER2- advanced or metastatic breast cancer [FDA. Verzenio Prescribing Information. Available from: https://www.accessdata.fda.gov/drugsatfda_docs/label/2017/208716s000lbl.pdf]. All are orally administered and act as selective ATP competitive inhibitors of CDK4 and CDK6, exhibiting little or no effect on other CDK.

Structurally, palbociclib and ribociclib are analogous [126] and show high specificity for CDK4 with an IC50 (half maximal inhibitory concentration) of 11 nM and for CDK6 with an IC50 of 16 nM [127, 128]. Abemaciclib has a different structure and a higher CDK4/6 binding activity than the other two drugs, with an IC50 of 2 and 10 nM for CDK4 and CDK6, respectively [129]. Moreover, palbociclib should be taken concomitantly with food because its effectiveness may be reduced with an empty stomach [130]; conversely, the exposure of ribociclib and abemaciclib is not influenced by food intake. More consideration will be reserved in the next section to palbociclib that is the CDK4/6 inhibitor used in the thesis project.

Several randomized clinical trials have proved efficacy and safety of these CDK4/6 inhibitors and favored their approval. Ribociclib is the second CDK4/6 inhibitor that was approved based on the results of the phase III studies MONALEESA-2 and MONALEESA-3 comparing the combination of ribociclib plus letrozole and ribociclib plus fulvestrant versus placebo plus letrozole or fulvestrant alone, respectively [131, 132], and showing a significantly high progression free survival (PFS) in the combination groups. More recently, the phase III clinical trial MONALEESA-7 revealed a considerable prolongation in both PFS and OS in

premenopausal patients with ER+/HER2- breast cancer receiving a combination of ribociclib, ET, and goserelin [133]. Ribociclib is recommended at a dose of 600 mg/day on a 3/1 schedule (3 weeks on/1 week off) and dose reduction is allowed if resistance does not occur [131]. Abemaciclib, the third CDK4/6 inhibitor approved, has been designed as monotherapy based on the outcome from the MONARCH-1 study showing a clinical benefit of the single agent in patients with pretreated refractory metastatic ER+ breast cancer [134]. In addition, worldwide phase III studies MONARCH-3 and MONARCH-2 evaluated the combination of abemaciclib with letrozole and fulvestrant in patients with ER+/HER2- metastatic breast cancer as first- and second-line therapy respectively, demonstrating a significantly improved PFS [135, 136]. Abemaciclib is administrated continuously twice daily at 150 mg if combined and at 200 mg as monotherapy [137].

Despite efficacy and tolerability shown by these drugs, they are not immune to side effects such as neutropenia that is the most dangerous [138-141]; therefore, two next-generation CDK4/6 inhibitors (i.e., G1T28 and G1T38) associated with lesser myelosuppression have been developed and are currently tested in clinical trials [142, 143].

3.2.1 Palbociclib

Palbociclib is the first highly selective ATP competitive CDK4/6 inhibitor synthesized and approved by FDA and EMA for the treatment of ER+/HER2- locally advanced or metastatic breast cancer in combination with AI in postmenopausal women as first-line therapy and in combination with fulvestrant in patients that were previously treated with ET [FDA. Ibrance Prescribing Information. Available from: https://www.accessdata.fda.gov/drugsatfda_docs/label/2017/207103s004lbl.pdf]. Palbociclib has been also approved by FDA for the treatment of ER+/HER2- metastatic male breast cancer [144]. The recommended dosing regimen consists of 125 mg/day of orally administrated drug on a 3/1 schedule (3 weeks on/1 week off) in combination with letrozole (2.5 mg/day) or fulvestrant (500 mg/month intramuscularly injected) and, if resistance does not occur, doses can be reduced to 100 or up to 75 mg/day [FDA. Ibrance Prescribing Information. Available from: https://www.accessdata.fda.gov/drugsatfda_docs/label/2017/207103s004lbl.pdf].

ER+ breast cancers are characterized by high expression of the ER-dependent gene cyclin D1 (*CCND1*) that mediates cell cycle entry through CDK4/6 by the phosphorylation and subsequent inactivation of Rb that uncouples from E2F. The release of this transcriptional factor promotes the transcription of genes involved in the G1/S checkpoint. Therefore, palbociclib inhibition of CDK4/6 decreases the E2F-dependent gene expression that regulates mitotic entry, thus suppressing DNA replication and causing a cell cycle arrest in the G1 phase [145, 146] (**Figure 9**). Consequently, the biological function and anti-tumoral effect of this drug are limited by the presence of an active Rb protein [127].

Palbociclib does not exert any effects on apoptosis [147] according to its cytostatic action. Additionally, palbociclib inactivates the transcription factor FOXM1 which is involved in the induction of cell division [57] and, besides the well characterized anti-proliferative effect, it has been shown to promote epithelial-mesenchymal transition (EMT) and tumor invasion [148].

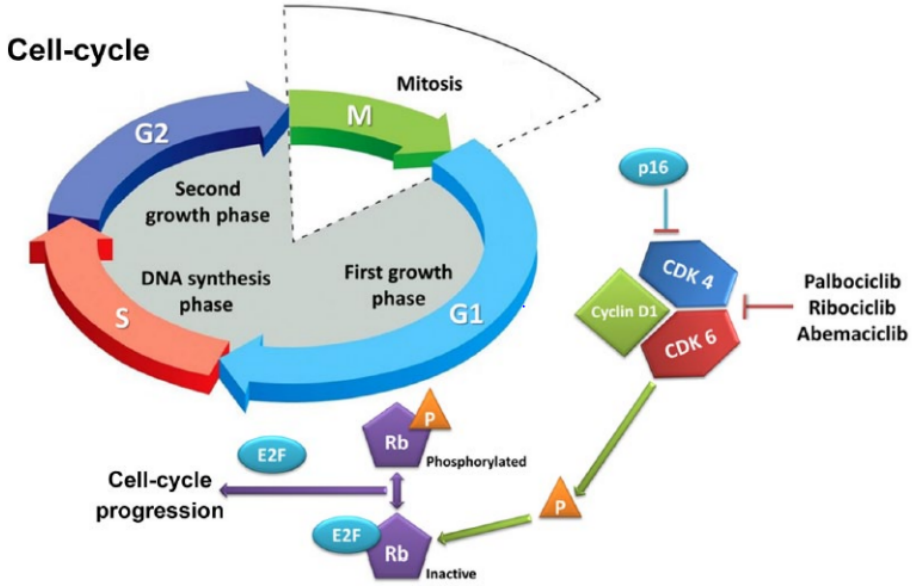

Figure 9. Mechanism of action of CDK4/6 inhibitors (taken from [149]).

Palbociclib anti-tumoral effect has been validated in several human cancers such as hepatocellular carcinoma [146], neuroblastoma [150], pancreatic ductal adenocarcinoma [148], melanoma [151], and especially breast cancer [152]. Three pivotal randomized clinical trials have allowed palbociclib entry into the clinic. PALOMA-1 and PALOMA-2 are phase II and phase III trials that proved efficacy and safety of palbociclib in combination with letrozole versus letrozole alone as firs-line therapy in the postmenopausal metastatic setting, showing a significant prolongation in the PFS [138, 153]. PALOMA-3 is a phase III study that investigated the combination of palbociclib plus fulvestrant versus fulvestrant alone in pre and postmenopausal women with disease progression during or after prior hormonal therapy and exhibited improved efficacy over ET alone [154].

The clinical efficacy of palbociclib has been explored also in the neo-adjuvant setting and in HER2+ breast cancer. NeoPalAna is a single-arm phase II study testing the combination of anastrozole plus palbociclib in stage II/III ER+ breast cancer. The trial showed a significantly higher complete cell cycle arrest (CCCA) than monotherapy [155]. The phase II trial NA-PHER2 investigated the combination of palbociclib, fulvestrant, and trastuzumab in the neo-adjuvant setting in women with ER+/HER2+ breast cancer and showed a complete pathological response in the combination arm [156]. The combination of palbociclib plus trastuzumab has already demonstrated a synergistic effect in human breast cancer cell lines [157] and both CDK4 and cyclin D1 are required for murine breast cancer growth [158-160]. Therefore, further

investigations on the clinical benefit of combining CDK4/6 inhibitors and anti-HER2 therapy are needed and many clinical trials are ongoing: e.g., the phase II PATRICIA study (evaluating palbociclib plus trastuzumab ± letrozole; NCT02448420), the phase III PATINA study (assessing efficacy of anti-HER2 therapy ± palbociclib; NCT02947685), and the phase II monarcHER study (evaluating abemaciclib plus trastuzumab ± fulvestrant; NCT02675231).
The main side effect related to palbociclib administration is neutropenia together with fatigue, nausea, alopecia, diarrhea, and anemia. Results from clinical trials also indicate that *de novo* or acquired resistance could emerge also for this treatment and investigating the molecular and metabolic mechanisms underlying such resistance is an important need.

4. Therapy resistance

Despite numerous advances in early detection and insights in the molecular mechanisms of breast cancer biology, some patients with early-stage breast cancer show *de novo* and/or acquired resistance.
Drug resistance can occur through different mechanisms, including multi-drug resistance, alteration in drug metabolism and efflux, cell death preventing, metabolic reprogramming, epigenetic changes, enhancing DNA repair, gene mutations and target modulations, crosstalk between cancer cells and microenvironmental factors.
Intrinsic or acquired resistance to anti-cancer therapy is an important problem that limits the use in the clinical setting. Innovative agents and combination strategies together with standard regimens need to be investigated to combat or delay the onset of recurrence, and predictive biomarkers of resistance should be identified to select patients that may benefit from a specific therapy.

4.1 Endocrine therapy resistance

Despite the relative safety and efficacy of the endocrine agents in improving prognosis of ER+ breast cancer patients, tumor cells can develop therapy resistance. Unfortunately, not all patients respond to the first endocrine manipulation and around 30% of women who initially respond would later relapse with acquired resistance [161].
Specifically, a third of tamoxifen treated patients with early-stage breast cancer may be refractory within 2-5 years or display *de novo* resistance to the initiation treatment [162]. Furthermore, long-term exposure to tamoxifen in postmenopausal women correlates with enhanced risk of endometrial cancer due to its agonistic activity. Letrozole and fulvestrant can be used as alternatives to replace tamoxifen in the first-line setting and, particularly, as second-line therapeutic options, delaying the emergence of ET resistance in postmenopausal patients

[163]. Numerous clinical trials suggest that AI show greater anti-tumoral efficacy than tamoxifen and may be effective in tamoxifen resistant patients [164]. Moreover, fulvestrant alone or combined with letrozole can also delay the emergence of acquired resistance in postmenopausal women. However, despite the initial success of a positive response to the treatment, resistance to AI and fulvestrant could also occur [161] and understanding the underlying mechanisms that drive ET resistance is indispensable to discover predictive markers and/or alternative targets to develop definitive approaches for preventing or overcoming resistance.

Cumulative data show that several mechanisms are associated with ET resistance. Importantly, a large body of literature describes the intricated crosstalk between ER and GF receptors, loss and mutations occurring on *ESR1* and related coregulators, cell cycle checkpoint alterations, enhanced autophagy, epigenetic aberrations and the controversial role of microRNA (miRNA) [165, 166] (**Figure 10**).

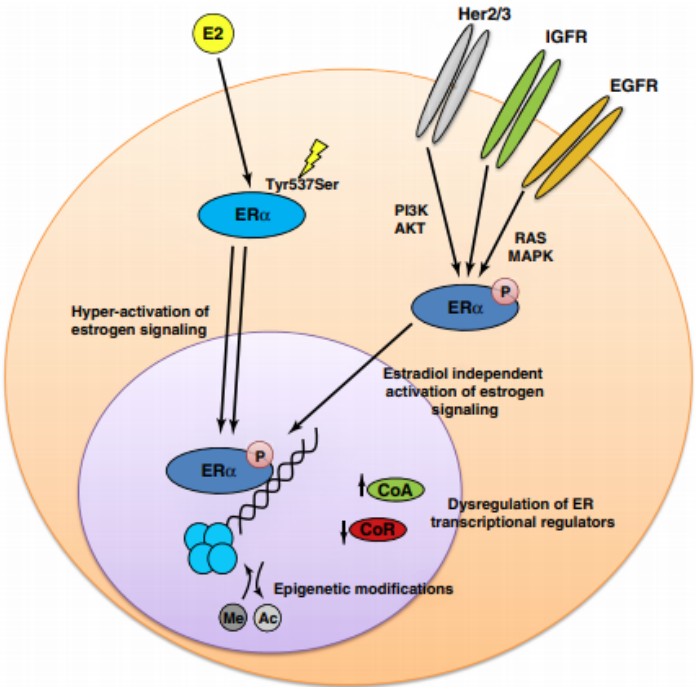

Figure 10. Schematic representation of the principal molecular mechanisms underlying endocrine resistance in ER+ breast cancer (taken from [165]).

4.1.1 Crosstalk between estrogen receptor and growth factor receptors

Although ER status is a reliable indicator of ET response, both preclinical and clinical studies indicate that HER2 overexpression and/or amplification confers resistance to ET, even in the presence of hormonal receptors [167]. HER2 is a member of the tyrosine kinase receptor (RTK) superfamily (i.e., EGFR superfamily) and its overexpression and/or aberrant activation approximately occurs in 30% of metastatic breast cancers, associated with decreased PFS and OS, and poor outcome in tamoxifen treated patients [168]. Indeed, an *in vivo* study has

demonstrated that HER2 crosstalks with the ER coactivator A1B1 enhancing the agonistic action of the tamoxifen-ER complex [169].

Accordingly, several reports confirm the existence of a bidirectional crosstalk between ER and RTK that can modulate the response to ET. In particular, overexpression and/or amplification of GF receptors, such as FGFR1 (fibroblast growth factor receptor one), IGF1R, and RET (rearranged during transfection), are implicated in the onset of ET resistance. Their signaling pathways converge on the downstream kinases including ERK1/2, MAPK, PI3K, and AKT which can phosphorylate ER (e.g., on ser118), triggering its ligand-independent activation and altering the response to different endocrine agents [170-173].

Importantly, *PIK3CA* gene is mutated in ~40% of human breast cancers [174] and its aberrant activation has been clinically exploited with a range of compounds targeting PI3K pathway such as inhibitors of mTOR, a serine/threonine kinase that is the major and most studied downstream effector of the PI3K/ATK pathway, involved in important cellular processes, such as protein synthesis and cellular metabolism [175]. Therefore, mTOR has become an attractive target to revert ET resistance. The randomized phase III trial BOLERO2 has shown that the combination of the mTOR inhibitor everolimus with the AI exemestane improves PFS in ER+ breast cancer patients previously treated with a nonsteroidal AI [176] but can also induce toxicity issues. However, several evidence from preclinical and clinical studies propose the targeting of both ER and GF pathways as a promising approach to overcome endocrine resistance.

4.1.2 Cell cycle checkpoint alterations

Both normal and tumor cells receive a plethora of proliferative and anti-proliferative signals and the balance between these inputs defines the cell cycle access or the entrance in a quiescent phase [177]. Deregulated cell cycle progression and checkpoints can also contribute to ET resistance [178].

Several studies have shown that the overexpression of positive cell cycle regulators causing a massive activation of CDK contributes to the development of endocrine resistance. Many tumors increase cyclin D-dependent activities, thereby escaping senescence and sustaining aggressiveness via multiple mechanisms such as CDK4 or CDK6 amplification and mutations, cyclin D1 translocation, amplification, or overexpression [179].

Cyclin D1 amplification is a common event in ER+ breast cancer, identified in 58% of luminal B breast cancers and 29% of luminal A tumors [180]. Anti-estrogen-induced growth arrest in ER+ breast cancer cells is sustained by decreased levels of cyclin D1, whereas a persistent cyclin D1 expression and the subsequent Rb phosphorylation characterize ET resistant cells [181, 182]. Besides regulating the cell cycle, cyclin D1 could interact with a number of transcription factors, including ER and STAT3 (signal transducer and activator of transcription three) [183]. It has been reported that tamoxifen promotes cyclin D1 binding to ER thus activating both STAT3 and ER. In this way, cyclin D1 overexpression may affect tamoxifen response [184]. In view of

the importance of cyclin D1 in mediating endocrine resistance, several clinical trials have evaluated the use of CDK4/6 inhibitors in combination with ET leading to their approval for the treatment of ER+/HER2- locally advanced or metastatic breast cancer, as previously described.
Additionally, overexpression of c-Myc and cyclin E1 or decreased expression of CDK inhibitors, p21 and p27, have been related to reduce sensitivity to ET [185]. Moreover, estrogens and the tyrosine kinase Src, which plays an important role in promoting survival and proliferation, inhibit the activity of p27, thus preventing the cell cycle arrest [186]. Finally, increased expression of miRNA such as miR-221 and miR-222 has also been proven to reduce the expression of p27 ultimately supporting tamoxifen resistance [187].

4.1.3 Autophagy

Autophagy is an intracellular lysosomal self-digestion process leading to the fusion of damaged or unnecessary subcellular components with lysosomes and to their subsequent degradation. This pathway is responsible for the quality control of essential cellular organelles and is crucial for homeostasis and survival of normal and cancer cells during stress conditions such as nutrient deprivation [188].
An important study demonstrated that autophagy inhibition induces ET sensitivity restoration, promoting cell apoptosis in preclinical models of ER+ breast cancer [189]. The complete mechanism of the autophagy-mediated resistance is still not fully understood but also *in vivo* models showed that autophagy inhibitors may restore anti-estrogen sensitivity in resistant tumors [190].
Autophagy inhibition is currently explored in early phase trials in breast cancer patients resistant to ET and hydroxychloroquine (HCQ), that together with chloroquine (CQ) is the only autophagy inhibitor available in the clinic, has been evaluated in metastatic ER+ breast cancer progressing on hormonal therapy in a phase I study
[https://www.mycancergenome.org/content/clinical_trials/NCT02414776/].

4.2 Cyclin-dependent kinases 4/6 inhibitor resistance

As mentioned above, the CDK4/6 inhibitor addition to the standard endocrine therapy has offered improved prognosis to patients with ER+/HER2- locally advanced or metastatic breast cancer. However, not all patients respond to the first-line treatment showing *de novo* resistance and most women who greatly benefit from CDK4/6 inhibition might develop acquired resistance [191]. Various mechanisms responsible for the emerging issue of intrinsic or acquired resistance have been proposed (**Figure 11**) but no predictive biomarkers have been yet identified.

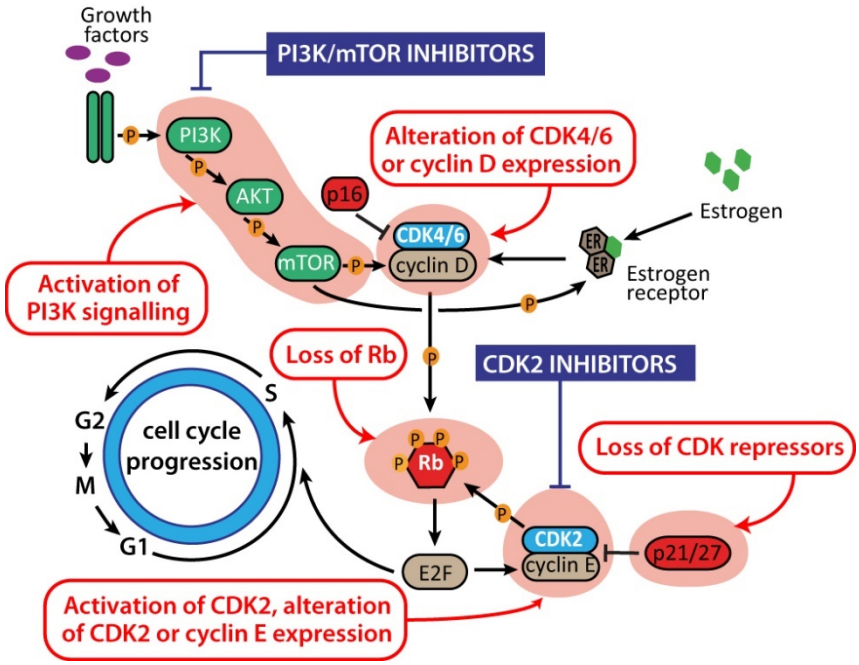

Figure 11. Schematic representation of the principal molecular mechanisms underlying CDK4/6 inhibitor resistance (adapted from [192]).

The tumor suppressor Rb is the main target of CDK4/6 representing one of the most promising biomarkers of therapy sensitivity [193, 194]. Various preclinical studies support the loss of Rb as a cause of CDK4/6 inhibitor resistance [195, 196]. Indeed, it has been reported that CDK4/6 inhibitors effectively arrest the cell cycle in Rb positive human cancers both *in vitro* and *in vivo* while showing no effect in Rb negative tumors [127, 145, 157, 197]. The role of Rb status has been also confirmed in a panel of breast cancer cell lines where higher levels are identified in the sensitive group [157] and in an *ex vivo* model of breast cancer in which Rb loss is related to therapy response failure [197]. Moreover, mutations in *Rb* gene have been detected in palbociclib or ribociclib treated patients with progressed metastatic breast cancer and were identified as responsible for the onset of the acquired resistance [198, 199]. However, Rb is not the only determinant of CDK4/6 inhibitor resistance since cell lines with detectable expression of Rb have shown a resistant phenotype and, on the other hand, cells that show Rb loss may still respond to therapy [145, 157].

The combination of *CCND1* amplification and loss of *p16INK4a*, a tumor suppressor involved in the cell cycle regulation through the CDK4 inhibition, has emerged as biomarker of sensitivity to CDK4/6 inhibitors [157, 197, 200, 201] both in the presence and absence of Rb loss. However, loss of *p16/CCND1* amplification did not show any significant clinical benefits in any of the PALOMA studies [141, 202] and their use as biomarkers for patient selection is still controversial.

Although CDK4 is not commonly overexpressed in breast cancer, it has been reported that, together with CDK6 overexpression, may promote resistance in preclinical models [198, 203-205]. Palbociclib can efficiently arrest the proliferation of CDK6 highly expressing ER+ breast

cancer cells poorly responsive to fulvestrant but, in the clinical setting, high expression of CDK6 has been correlated with reduced PFS [206]. Such potential role of CDK6 overexpression in conferring resistance might be due to its kinase-independent functions such as the upregulation of p16 and VEGFA [207, 208].

The complex cyclin E/CDK2 can also promote the release of E2F via Rb phosphorylation allowing cell entry in the S phase [209]. Thus, in the presence of prolonged CDK4/6 inhibition, the cyclin E/CDK2 axis may be a crucial bypass mechanism for the resistant cells to escape from the cell cycle arrest [145]. Indeed, overexpression of *CCNE1* attenuates the inhibitory effect of palbociclib and is involved in the acquisition of resistance. Targeting CDK2 in combination with CDK4/6 may be a successful strategy to overcome resistance [195, 210]. Also in the clinical setting, *CCNE1* highly expressing patients from the PALOMA-3 study showed a shorter PFS after the combination treatment of palbociclib plus fulvestrant [211].

Other cell cycle specific mechanisms of resistance to CDK4/6 inhibitors include: (i) overexpression of the transcription factor E2F [145], the cell cycle regulator CDK7 [212], WEE1 that plays an important role in the G2/M checkpoint, and MDM2 (Mouse Double Minute two homolog), a protein that negatively regulates p53 [212]; (ii) HDAC activation that suppresses the natural CDK inhibitor p21 by removing acetyl groups [213]; (iii) loss of FZR1 (fizzy-related protein homolog one) which functions as an activator of APC/C regulating G1/S checkpoint and late mitosis [58, 214] (**Figure 12**).

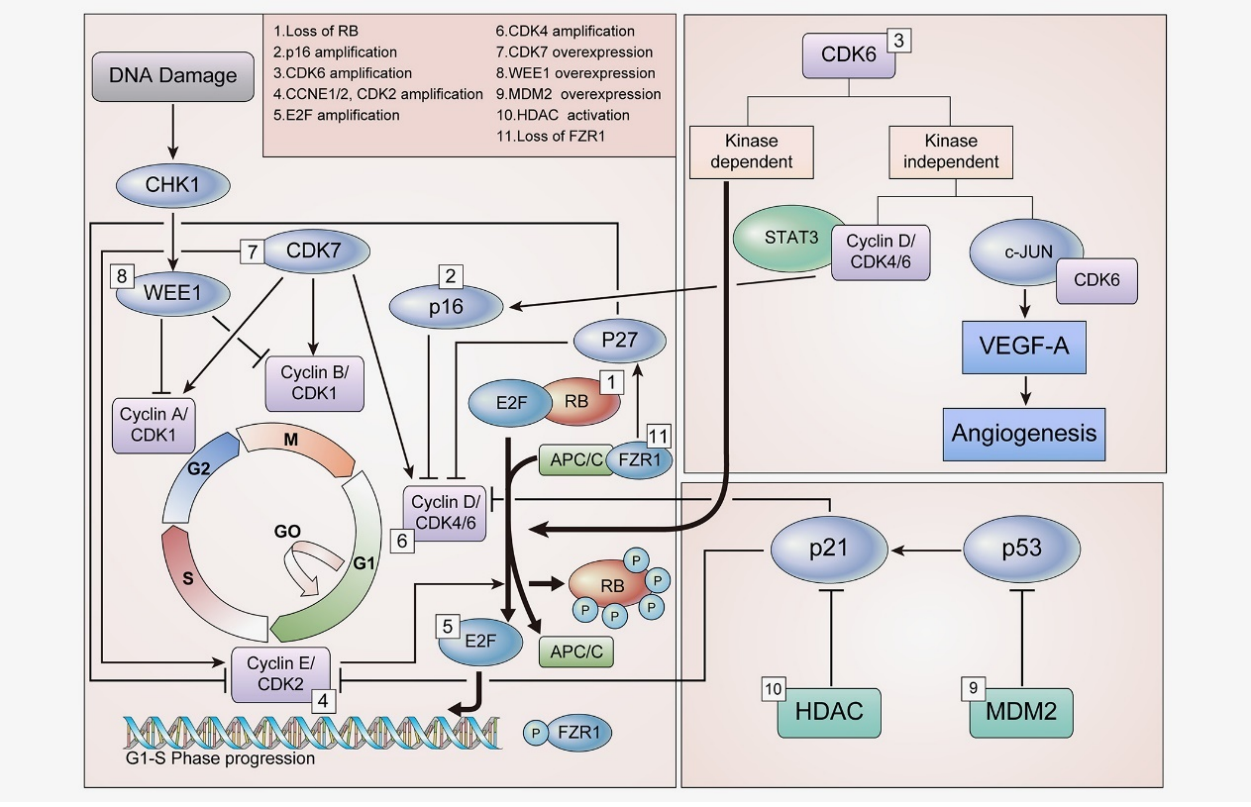

Figure 12. Cell cycle-related mechanisms of resistance to CDK4/6 inhibitors (taken from [212]).

Some cell cycle non-specific mechanisms of CDK4/6 inhibitor resistance have also been identified (**Figure 13**). Loss of ER and *ESR1* mutations have been correlated with AI resistance in breast cancer [215] and, more recently, it has been reported that loss of ER may also drive abemaciclib resistance [203]. The role of CDK4/6 inhibitors in breast cancer cells harboring *ESR1* mutations is still controversial and need to be further investigated [216, 217].

The FGFR signaling pathway exerts a key role in proliferation, survival, differentiation, and also cancer progression. Importantly, *FGFR1* overexpression as well as *FGFR2* activating mutations can contribute to the development of resistance to CDK4/6 inhibitors and SERD [218, 219].

A correlation between CDK4/6 and the PI3K/AKT/mTOR signaling pathway, that is activated in many ER+ breast cancers [195, 220] due to *PIK3CA* mutation or loss of *PTEN*, has been reported as bypass mechanism to overcome therapy resistance. The uncanonical activation of the cyclin D1/CDK2 complex can promote the recovery of cyclin E expression which in turn sustains S phase entry despite the CDK4/6 inhibition. The inhibition of PI3K impairs cyclin D1 expression levels and prevents the adaptation to the therapy [195]. In addition, the downstream effector PDK1 (3-phosphoinositide-dependent protein kinase 1), that is required for the full activation of AKT, is involved in ribociclib resistance. Both pharmacological and genetic inhibition of PDK1, mTOR or CDK2 in combination with ribociclib can re-sensitize cells to CDK4/6 inhibitor [221].

Additional cell cycle nonspecific mechanisms of resistance to CDK4/6 inhibitors are (i) the higher transcriptional activity of AP1 that regulates a variety of genes such as *CCND1* [212]; (ii) the TGFβ-induced EMT via SMAD pathway or PI3K/AKT/mTOR signaling [148, 222, 223]; and (iii) immune-related pathways such as those of interferon (IFN)-α and -β that have been found enriched in breast cancer cellular models resistant to CDK4/6 inhibitors [212].

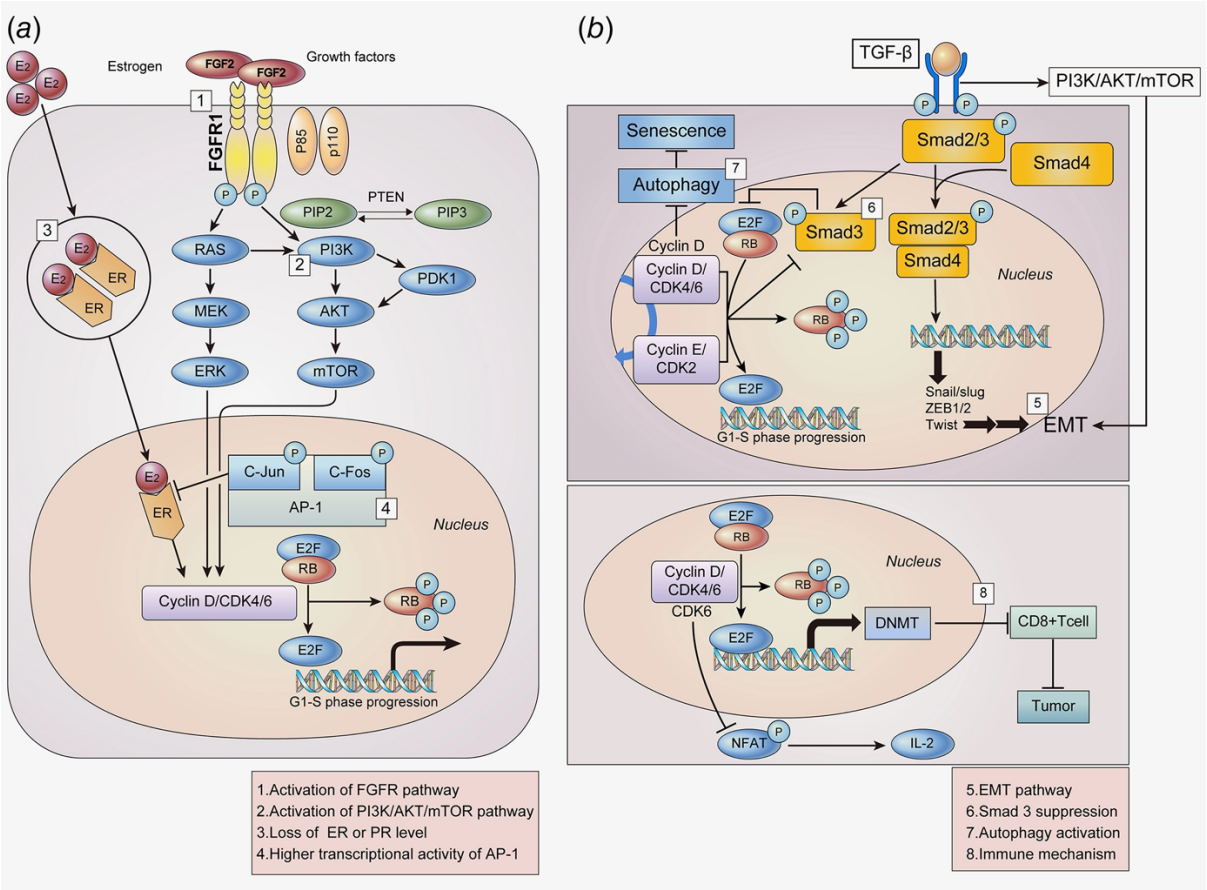

Figure 13. Cell cycle nonspecific mechanisms of resistance to CDK4/6 inhibitors (taken from [212]).

More recently, it has emerged that also the metabolic adaptation could underlie such resistance. For example, CDK4/6 inhibition may activate autophagy that reverts the cell cycle arrest. Combination of CDK4/6 and autophagy inhibition exerts, therefore, a synergic effect in blocking tumor growth [224]. Additionally, we have demonstrated that $ER^+/HER2^-$ and $ER^+/HER2^+$ palbociclib resistant breast cancer cell lines show a different glucose-dependent catabolism. While $ER^+/HER2^-$ breast cancer cells display increased aerobic glycolysis when sensitive, $ER^+/HER2^+$ cells improve their glycolytic dependency at the time of palbociclib resistance. Hence, targeting glucose metabolism can re-sensitize $ER^+/HER2^+$ resistant cells to palbociclib and significantly increase its anti-tumoral effect in $ER^+/HER2^-$ sensitive cells [225]. Of note, in esophageal squamous cell carcinoma, cyclin D1 overexpression or loss of its regulatory E3 ubiquitin ligase Fbxo4 (F-box protein 4) result in glutamine addiction and mitochondrial dysfunction thus reducing energy production. The combination of a glutaminase 1 (GLS, the enzyme that generates glutamate from glutamine) inhibitor plus the mitochondrial complex I inhibitor metformin affects the survival of cells resistant to CDK4/6 inhibitors [226].

Despite evidence collected from preclinical studies suggest that several mechanisms may contribute to intrinsic or acquired resistance to these agents, no potential biomarkers have been clinically validated. Currently, ER positivity and HER2 negativity are the only biomarkers

available and further investigations are needed to propose combination strategies successful in overcoming drug resistance and to select patients and personalize treatment.

5. Tumor metabolism

Tumor initiation, progression, and metastasis are characterized by alterations arising in multiple signaling pathways involved in the regulation of physiological functions (e.g., growth, proliferation, differentiation, survival, DNA repair, and apoptosis) and allowing cells to bypass the typical checkpoints required for normal cell division. Oncogene and tumor suppressor mutations render the cancer genomic landscape highly complex and heterogeneous [227] and widely affect cancer metabolism.

Tumor metabolic reprogramming is an established trait of cancer (**Figure 14**) and is essential not only to satisfy the anabolic and energetic demands of highly proliferating cancer cells but also to promote invasion, metastasis, therapy resistance, and other cellular processes involved in the malignant transformation. This adjustment in their metabolic behavior confers to cancer cells the ability to survive and adapt under stress conditions such as nutrient starvation, hypoxia, or drug-induced cytotoxicity [228]. Tumor metabolic reprogramming comes from both oncogenic signaling pathways and environmental factors. Indeed, cancer cells are surrounded by different cellular components of the tumor microenvironment, which can influence cancer metabolism by exerting an additional selective pressure on tumor cells to adapt to such unsuitable conditions.

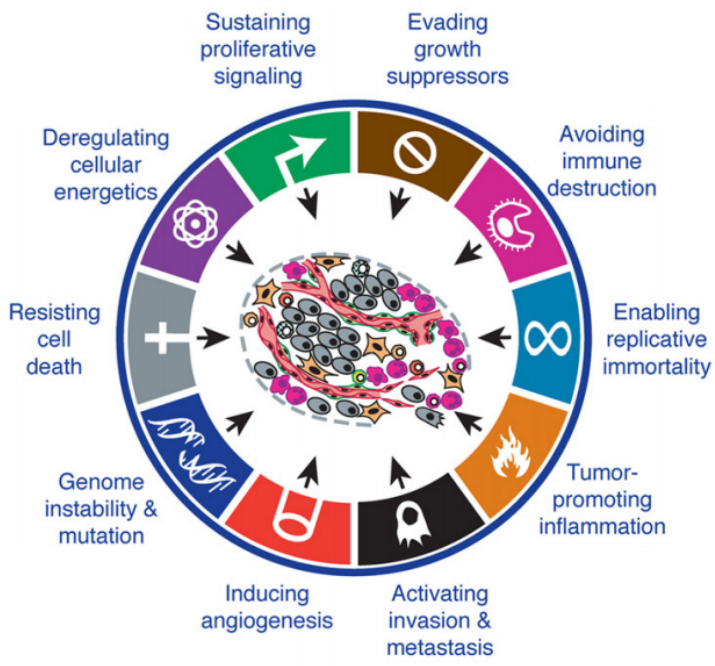

Figure 14. The hallmarks of cancer: the next generation (adapted from [229]).

5.1 Glucose metabolism

A well-characterized deregulation in cancer metabolism is the large consume of glucose to facilitate biomass production (e.g., amino acids, lipids, nucleotides) by providing glycolytic intermediates even in the presence of oxygen. This phenomenon is currently referred to as aerobic glycolysis or Warburg effect [230] and represents a crucial metabolic divergence between tumor and normal cells (**Figure 15**). Indeed, normally differentiated cells usually rely on the mitochondrial function to meet the energetic demand in conditions with sufficient oxygen, through three differentially compartmentalized processes: glycolysis, which metabolizes glucose into pyruvate and takes place into the cytoplasm, the tricarboxylic acid (TCA) or Krebs cycle and the subsequent oxidative phosphorylation (OXPHOS) diverting pyruvate in form of acetyl-coenzyme A (acetyl-CoA) into the mitochondria where it is completely oxidized to CO_2 to approximately generate 36 molecules of ATP (adenosine 5'-triphosphate). Oxygen is essential for this process because it represents the electron acceptor required for glucose oxidation. Conversely, under hypoxic conditions, normal cells use glycolysis and lactic fermentation for energy supply thus producing only two net ATP molecules while consuming NADH (nicotinamide adenine dinucleotide) in a process known as anaerobic glycolysis.

In contrast, proliferating cancer cells mainly depend on glycolysis and subsequent fermentation of glucose into lactate even in the presence of abundant amount of oxygen [230]. Several hypotheses have been formulated and Warburg and colleagues concluded that this phenomenon was due to defective mitochondria leading to an impaired aerobic respiration and to the consequent reliance on glycolytic metabolism [230]. However, later studies reported that the mitochondrial function was not damaged in most cancer cells [231-233] and, although tumors usually suppress mitochondrial oxidative phosphorylation even in normoxic condition, this does not mean that cancer cells lose their ability of fully oxidating glucose. A potential plausible explanation is the need of rapid ATP generation. Indeed, although the ATP production efficiency is lower in Warburg metabolism, the yield rate is faster than OXPHOS; therefore, higher amount of ATP molecules are generated from aerobic glycolysis to meet the increasing energetic and anabolic demand to support rapid tumor progression [228, 234].

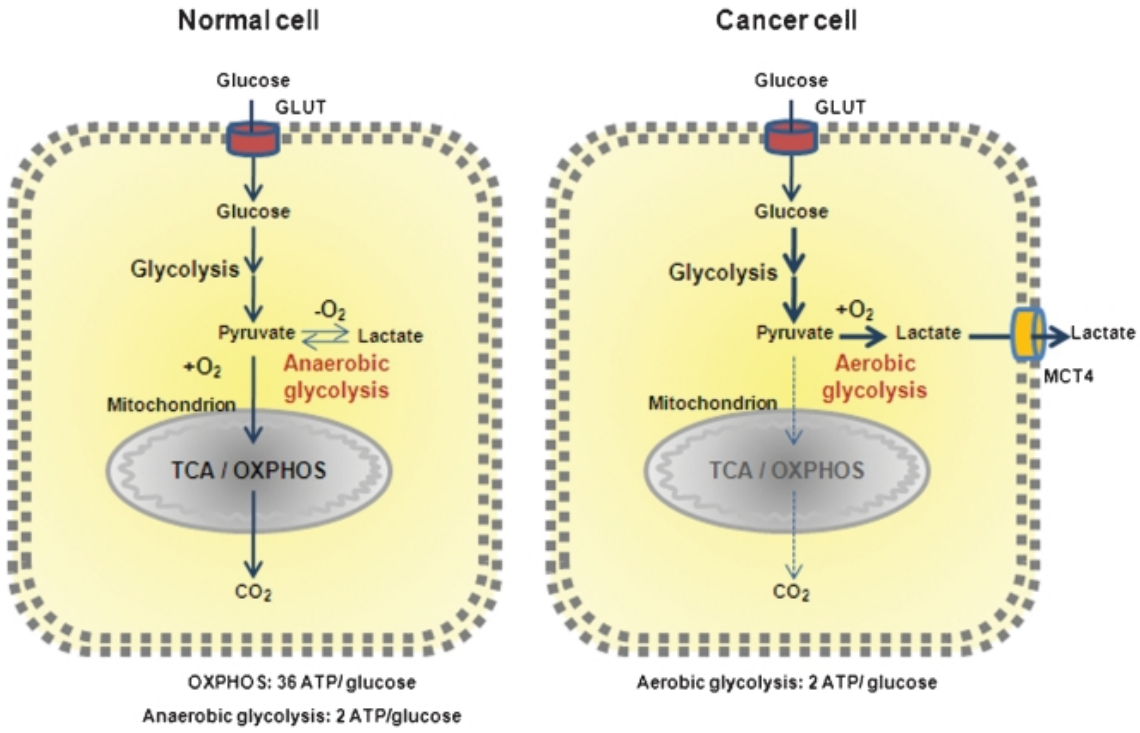

Figure 15. Metabolic comparison between normal and cancer cells (taken from [235]).

This highly glycolytic rate provides several advantages to proliferating cancer cells. In addition to the faster energy production that can exceed the amount of ATP generated by OXPHOS, the Warburg effect ensures a substantial increase in tumor biomass, necessary for biosynthetic processes sustaining proliferation. Indeed, the enhanced rate of glucose uptake and consumption through glycolysis leads to a consistent number of carbons resulting in essential sources available for anabolic processes including *de novo* biosynthesis of nucleotides, proteins, and lipids.

The accumulation of glycolytic intermediates is directly connected to the pentose phosphate pathway (PPP) which generates ribose-5-phosphate for nucleotide biosynthesis and NADPH as reducing power for biosynthetic reactions (e.g., lipogenesis) and as cofactor of antioxidant enzymes such as GSH, that is a major intracellular defense against ROS-mediated damage [236]. Glucose degradation and intermediate production also provide glycerol and citrate useful for lipid biosynthesis. Furthermore, glucose derived from the increased upload can be exploited to implement *de novo* serine biosynthesis to generate amino acids and one carbon units required for nucleotide biosynthesis, starting from the glycolytic intermediate 3-phosphoglycerate [236] (**Figure 16**).

In addition, the abnormal aerobic glycolysis of tumor cells favors the secretion of large amount of lactate via mono-carboxylate transporters (e.g., MCT1 and MCT4). MCT1 is frequently exploited by oxidative tumors to upload exogenous lactate released in the tumor microenvironment by glycolytic cells and metabolized through OXPHOS [237]. Conversely, MCT4 is predominantly used for lactate extrusion from glycolytic tumor cells [238]. The acidification of the surrounding microenvironment facilitates the release and subsequent

activation of proteolytic enzymes and metalloproteases involved in the degradation of the extracellular matrix and promotes cancer invasion and metastasis [239] while increasing the extracellular levels of VEGFA, thus sustaining tumor angiogenesis and progression [240]. Furthermore, the lowering effect of the lactic acid on the intratumoral pH levels also damages the peritumoral normal cells, which could not counteract the acidosis-induced apoptosis [241, 242]. Finally, lactic fermentation allows the regeneration of NAD+, necessary for maintaining an active glycolytic flux.

By providing carbon units for lipid, protein, and nucleotide biosynthesis, the enhanced aerobic glycolysis is supported by an exclusive regulation of transporters and metabolic enzymes [243, 244]. Glucose uptake is regulated across the plasma membrane by glucose transporters (GLUT1-4). GLUT1 is the most overexpressed isoform in cancer and contributes to a substantial increase of glucose import into cytoplasm. GLUT1 higher expression correlates with poor prognosis in cancer patients [245]. GLUT1 is upregulated by oncogenes including c-Myc, K-Ras, and HIF1-α (Hypoxia-Inducible Factor 1-alpha) while tumor suppressors as p53 and PTEN (phosphatase and tensin homolog) are negative regulators [246, 247]. Glucose uptake and utilization by cancer cells have been successfully exploited in tumor patients through the introduction of the fluorodeoxyglucose-positron emission tomography (FDG-PET) imaging applied for cancer staging and therapy response monitoring [248, 249].

Hexokinase (HK) is the first rate-limiting enzyme of the glycolytic pathway catalyzing the phosphorylation of glucose to glucose-6-phosphate (G6P) and is allosterically and negatively regulated by its own product G6P. Five hexokinase isoforms exist (HK1-4 and the less characterized HKDC1) and HK2 has found upregulated in cancer. In this context, HK2 drives the uncoupling of glycolysis from OXPHOS thus sustaining the glucose flux into different metabolic pathways required for cellular transformation and carcinogenesis [250, 251].

To accumulate glycolytic intermediates and boost biomass production, cancer cells not only enhance glucose uptake, but also attenuate the conversion of phosphoenolpyruvate (PEP) into pyruvate that is the last glycolytic step catalyzed by PK enzyme with the concomitant phosphorylation of ADP (adenosine diphosphate) to ATP. PKM1 and PKM2 isoforms are encoded by the same gene as result of an alternative splicing: PKM1 is expressed in adult and differentiated cells whereas PKM2 predominates in embryonic, stem, and cancer cells [252-254]. PKM2 is upregulated in cancer, particularly breast and colon cancers [255, 256] and exerts its pro-tumorigenic effect becoming the predominant isoform over the constitutively activated PKM1. PKM2 can exist as high-activity tetramer or low-activity dimer that attenuates the last and irreversible step of glycolysis thus shuttling glycolytic intermediates into other anabolic pathways [253, 257-259]. Several factors control the switch between these two forms. Fructose-1,6-bisphosphate (FBP) and serine are positive regulators of the tetrameric PKM2 [260, 261]. In contrast, oxidative stress, tyrosine phosphorylation, and acetylation of lysine residues within PKM2 convert the tetrameric form into the less active dimeric form [262-264].

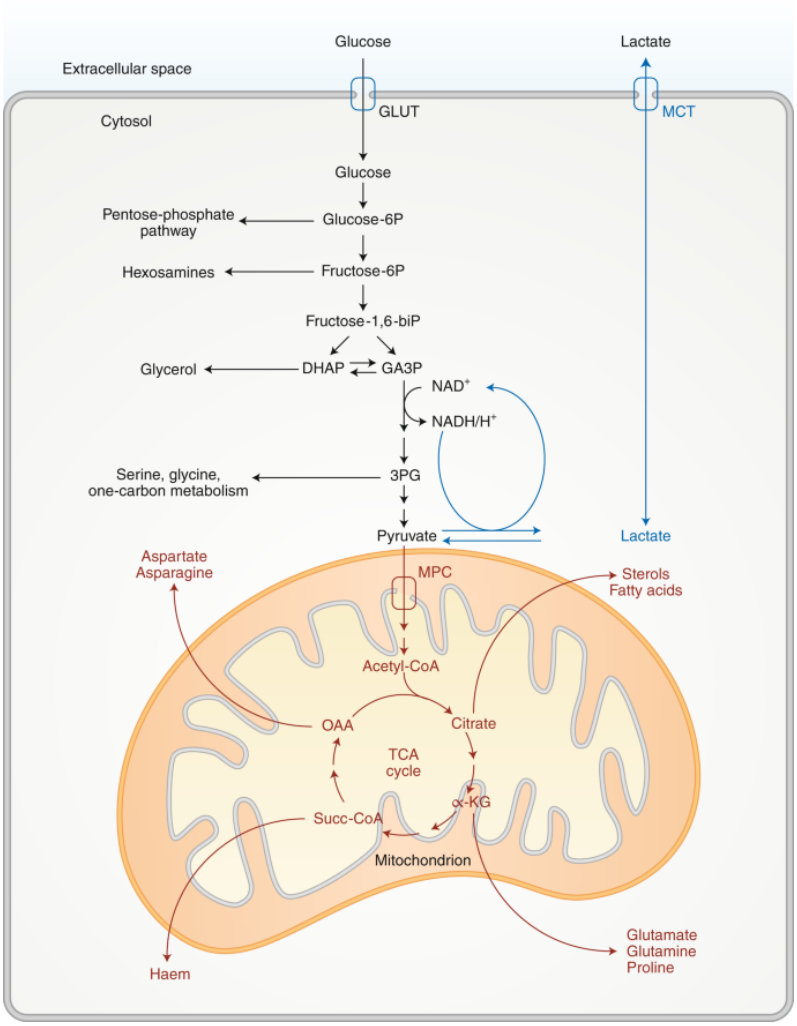

Figure 9. Reprogramming of glucose metabolism in cancer (taken from [265]).

Glucose uptake and catabolism in cancer cells are driven by altered transporters and enzymes, encoded by overexpressed or mutated oncogenes and tumor suppressor genes, as well as by regulators of hypoxia response. One connection between cancer and glucose metabolism is the PI3K/AKT/mTOR signaling pathway which coordinates the metabolic changes necessary to support tumor growth by increasing glucose intake and metabolism via various mechanisms.

PI3K signaling promotes GLUT1 transcription and localization at the plasma membrane [266, 267] and increases HK2, PFK1, and PFK2 activity [268, 269]. Furthermore, the downstream effector of PI3K/AKT pathway, mTOR, is crucial in cell growth, proliferation, and survival and positively regulates glucose metabolism [270, 271], thus representing an important therapeutic target in the clinic.

mTOR is an upstream activator of HIF1-α which in turn controls the expression of several genes involved in glucose metabolism. Indeed, HIF1-α upregulates glucose transporters (GLUT1 and GLUT3) and glycolytic enzymes (e.g., HK2, PFK1, PFK2, aldolase A and C, glyceraldehyde-3-phosphate dehydrogenase (GAPDH), enolase 1, PKM2) [272]. While in normoxic condition HIF1-α is degraded, cancer cells may display a stable HIF1-α activation even in the presence of oxygen [273-275], thus increasing the expression of GLUT1 and promoting the activation of

glycolytic enzymes such HK2 [276]. Furthermore, HIF1-α induces the expression of PDK1 (Pyruvate Dehydrogenase Kinase 1), which phosphorylates and inhibits the PDH (pyruvate dehydrogenase) complex [277, 278]. The inhibition of PDH impairs the pyruvate entry into TCA cycle and promotes its conversion into lactate catalyzed by LDH (lactate dehydrogenase). LDH is upregulated in different types of tumor and is related to an increased activity of HIF1-α and c-Myc [279].

Warburg effect is also regulated by oncogenes such as c-Myc and tumor suppressors as p53. c-Myc is an essential transcription factor involved in several important processes including proliferation, differentiation, apoptosis, and metabolism [280, 281] and c-Myc overexpression sustains tumorigenesis and cancer progression by inducing most of the glycolytic genes mentioned above [282]. Conversely, the tumor suppressor p53 is implicated in apoptosis, cell cycle regulation, and DNA damage sensing and it has been shown to counteract Warburg metabolism by decreasing the glycolytic flux and encouraging the mitochondrial respiration. Indeed, p53 represses the transcription of GLUT1 and GLUT4 and decreases PFK2 activity. Therefore, loss of p53 promotes glycolysis and anabolic biosynthetic processes in cancer cells [283].

This glucose metabolic reprogramming and the adaptation that occurs in cancer cells to support uncontrolled proliferation and fast growth can be exploited to develop inhibitors of metabolic enzymes and transporters for treating malignant tumors.

5.2 Amino acid metabolism

Besides the well characterized glucose metabolic reprogramming, highly proliferative cancer cells rely on other nutrients to meet the increased request of building blocks necessary for a rapid tumor growth. Similar to glucose, amino acid metabolism is regulated by oncogenes and tumor suppressors [246, 284-286] and has been reported to play important roles in tumor growth and survival.

Amino acids can be classified into two groups: non-essential amino acids, meaning that can be adequately synthesized endogenously (i.e., alanine, glutamate, glutamine, aspartate, asparagine, cysteine, glycine, proline, tyrosine, arginine, and serine) and essential amino acids that need to be taken from dietary sources (i.e., isoleucine, leucine, methionine, valine, phenylalanine, tryptophan, histidine, threonine, and lysine) and/or recycled from the autophagic degradation of dispensable proteins [287, 288].

In addition to be exploited as substrates for protein synthesis, amino acids can (i) work as metabolites and metabolic regulators, (ii) provide nitrogen for nucleotide biosynthesis and carbon for the TCA cycle to support energy metabolism and anabolic processes, (iii) maintain the redox balance (**Figure 10**).

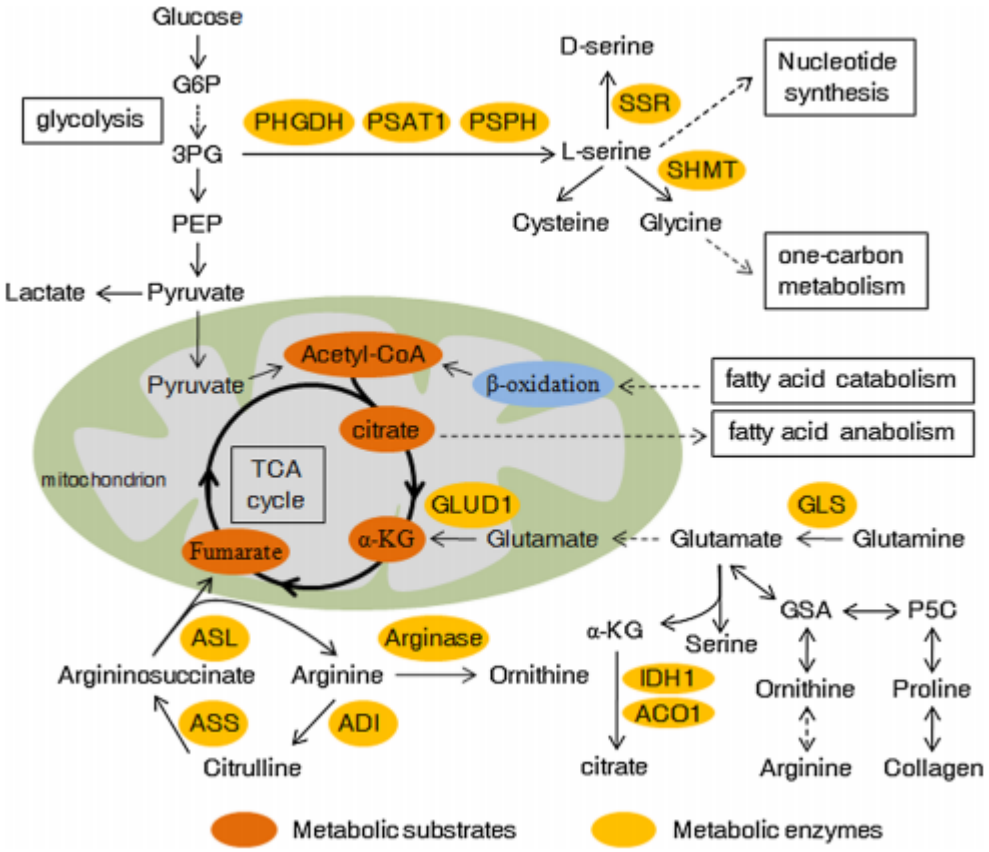

Figure 10. Amino acid metabolism and its crosstalk with other metabolic pathways (taken from [289]).

Glutamine is one of the non-essentials and the most abundant free amino acid in the cells, that is considered second only to glucose for importance in cancer. Glutamine is involved in energy production, signal transmission, catabolic and anabolic processes (e.g., the production of macromolecules such as proteins, lipids, and nucleotides) by providing nitrogen and carbon units, and in the maintenance of redox balance [290, 291]. Glutamine can be uploaded via plasma membrane transporters (e.g., SLC1A5 and SLC7A5) and then catabolized through a process called glutaminolysis consisting of the deamination of glutamine into glutamate, NAD(P)H, and ammonia catalyzed by GLS [292, 293]. GLS expression and glutamine catabolism are induced by the oncogenic c-Myc in cancer cells [284, 285] and by the tumor suppressor p53 at transcriptional level [294]. It has been reported that also the oncogenic K-Ras controls glutamine metabolic reprogramming in pancreatic cancer by inducing the upregulation of glutamate dehydrogenase (GDH) enzyme. Glutamate derived from glutaminolysis is then transferred into mitochondria and oxidized into alpha-ketoglutarate (α-KG) through a reaction known as oxidative deamination and catalyzed by GDH or via a transamination producing also nonessential amino acids [295]. α-KG can maintain the flow of the TCA cycle for producing anabolic carbons and energy via the electron transport chain (ETC) [296], a process known as anaplerosis.

Glutamine itself also provides nitrogen to produce hexosamines and some nonessential amino acids [297] and represents an alternative source of carbons for lipid production. Indeed,

glutamine derived α-KG can be reduced through a reductive carboxylation to citrate to sustain fatty acid (FA) biosynthesis [298]. It has been demonstrated that this reaction is crucial for cancer growth and progression [299-302].

Furthermore, glutamine is directly involved in nucleotide production by providing nitrogen pools that support *de novo* biosynthesis of purines and pyrimidines [303] and also maintains the redox balance by contributing to GSH synthesis [304, 305]. In addition, glutamine derived fumarate activates GPx1 (glutathione peroxidase) and Nrf2 (nuclear factor erythroid related factor 2) which are involved in ROS scavenging and anti-oxidative defense [306, 307]. Thus, glutamine metabolism is critical for cancer cell proliferation and survival [308, 309] and it has been shown that the inhibition of glutamine metabolism prevents tumor growth in breast cancer models [310].

Another fundamental amino acid is serine that can be imported from the extracellular microenvironment or *de novo* synthesized from glycolytic intermediates in a process where PHGDH (3-phosphoglycerate dehydrogenase) oxidizes 3-phosphoglycerate to 3-phosphohydroxypyruvate, that is a precursor subsequently transaminated and dephosphorylated to serine [311]. PHGDH has been found upregulated in several cancers including TNBC and is associated with poor prognosis [312]. The derived serine can be converted to glycine via SHMT (serine hydroxy-methyltransferase), generating one carbon molecules that are involved in the folate cycle and in the main downstream output of the folate cycle that is the nucleotide biosynthesis [313]. Serine- and glycine-fueled folate metabolism also contributes to NAPDH production and exerts a potential role in redox balancing and protection against oxidative stress [314-317]. In addition, serine and glycine act together as essential precursors of proteins, lipids, and nucleic acids, and glycine can donate methyl groups required not only for building block synthesis but also for DNA methylation. It has been demonstrated that tumor cell proliferation is supported by serine rather than glycine. Indeed, glycine supplementation does not replace serine in sustaining tumor cell growth since cancer cells specifically intake exogenous serine which is subsequently transformed into glycine to sustain building block synthesis [318].

Proline is a proteinogenic secondary amino acid, usually stored into collagen that is the most abundant protein in humans [319]. Proline synthesis starts from glutamate using 1-pyrroline-5-carboxylate (P5C) and glutamic-γ-semialdehyde (GSA) as intermediates. Proline dehydrogenase (PRODH) catalyzes the conversion of proline into P5C and acts as a mitochondrial tumor suppressor, induced by p53 and PPARγ (Peroxisome Proliferator-Activated Receptor gamma) and negatively regulated by c-Myc and miR-23b [320]. Additionally, GSA can be transformed in ornithine that is an arginine precursor in the urea cycle [321]. Proline metabolism has been related to cancer aggressiveness. Indeed, the overexpression of P5C reductase (PYCR), which converts P5C to proline, leads to excessive intracellular proline levels and reduced ROS thus promoting tumor progression [322].

Arginine is an essential amino acid that acts as nitrogen donor for nitric oxide (NO), as fuel for the urea cycle, and as precursor for proline, glutamate, and nucleotide biosynthesis. Argininosuccinate synthetase (ASS) is the rate-limiting enzyme of *de novo* arginine synthesis and converts acid aspartic and citrulline into argininosuccinate. Argininosuccinate lyase (ASL) catalyzes the production of arginine and fumarate linking arginine to energy metabolism via TCA cycle. Cancers lacking ASS are highly dependent on the exogenous amino acid for their proliferation [323] and have been shown to be susceptible to arginine deprivation therapy [324].
In conclusion, due to the important role of amino acids in cancer growth and aggressiveness, numerous efforts are focusing on the possibility to target amino acid metabolism via small molecule inhibitors.

6. Tumor metabolic reprogramming

Besides the importance of glycolysis in survival and progression of breast cancer, it has become increasingly evident that breast tumor cells may preferentially rely on alternative metabolic pathways to drive their aggressiveness. Several alterations dictate breast cancer metabolic reprogramming and plasticity and can be classified into cell-intrinsic and -extrinsic. The first are related to oncogenes and tumor suppressor genes that regulate metabolic pathways (e.g., PI3K/AKT/mTOR, c-Myc, p53) [325-328]; cell-extrinsic alterations include nutrient availability, hypoxia, acidosis, and the interaction with cellular components of the tumor microenvironment (e.g., fibroblasts, adipocytes, immune cells) that exert a selective pressure on cancer cells undergoing a favorable metabolic reprogramming in order to survive and metastasize. Furthermore, breast cancer cells may adopt a particular metabolic program based on their molecular subtype and understanding the metabolic reprogramming related to the different tumor subtypes as well as the underlying mechanisms is of fundamental importance to identify potential therapeutic vulnerabilities.
In ER+ breast cancer, E2 and ER have been shown to reprogram the metabolism based on glucose availability. In the presence of high amount of glucose, E2 improves glycolysis via enhanced AKT activity while limiting TCA cycle flow. Conversely, under hypoxic condition, E2 encourages TCA cycle exploitation to meet the increased energetic demand [329]. ER has also been shown to facilitate the transcription of HIF1-α that is upregulated under hypoxic stress and induces a glycolytic phenotype [330]. Thus, ER+ breast cancers are characterized by increased glycolysis, lactate secretion, and PPP flux, which fuel lipid and nucleotide biosynthesis, together with increased uptake of choline also involved in lipid biosynthesis. Additionally, the increased uptake of glycine and formate sustains the production of nucleotides and amino acids in hormone-dependent breast cancer. By contrast, ER- breast cancers exhibit a shift from glycolysis towards glutamine consumption to fuel TCA cycle as well as to provide nitrogen and

carbon units as precursors for proteinogenic amino acids and nucleotides (**Figure 11**) [331]. These observations suggest that TNBC breast cancers could benefit from GLS inhibitors or glutamine deprivation therapy, while ER+ tumors should be treated with glycolysis inhibitors [331].

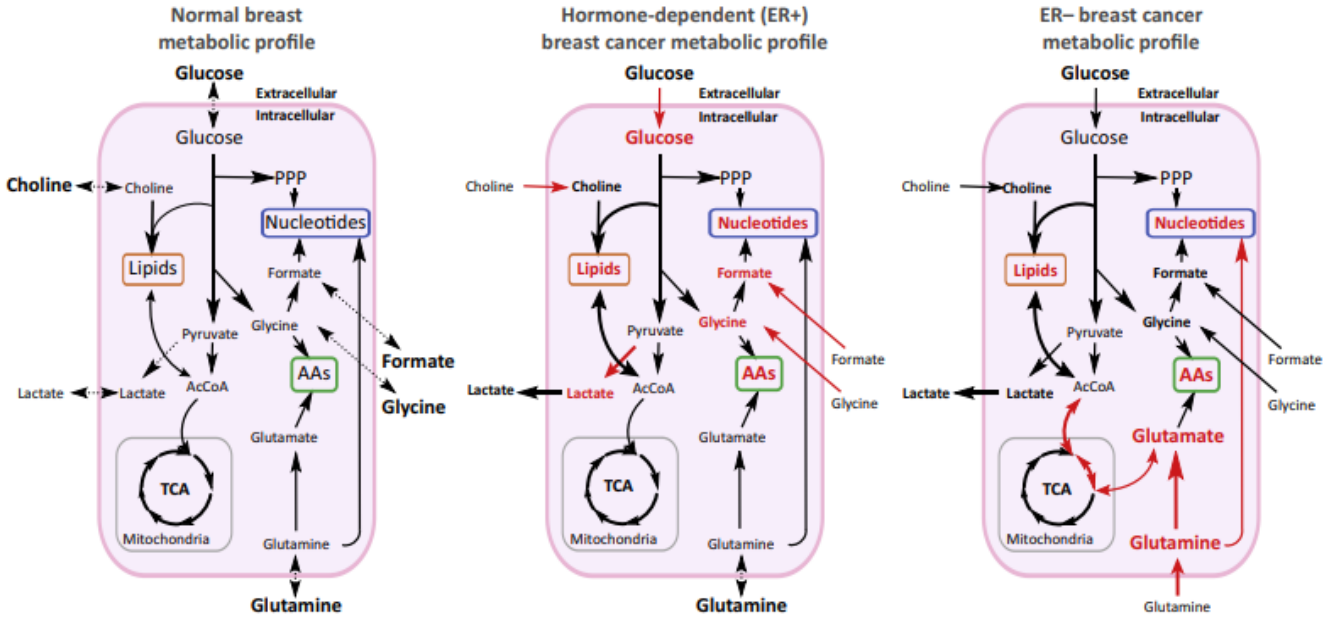

Figure 11. Metabolic alterations in hormone-dependent and -independent breast cancer (taken from [332]).

However, additional studies provided controversial data claiming that also TNBC and HER2+ breast cancers show increased rate of glycolysis and are characterized by the upregulation of glycolytic transporters and enzymes (e.g., GLUT1, HK2, and GAPDH) and PPP intermediates. Furthermore, recent findings have proven that TNBC rely on glucose metabolism more than luminal tumors and heavily depend on amino acid metabolism, especially on c-Myc-related serine, glycine, and tryptophan uptake [333]. Immunohistochemical staining of breast cancer tissues has revealed that HER2+ and TNBC are also characterized by higher expression of metabolic players related to glutamine metabolism, such as SLC1A5, GLS1, and GDH [334, 335]. Interestingly, TNBC display enhanced expression of carbonic anhydrase IX (CA IX), a tumor related protein involved in pH regulation and adaption to acidosis, causing further extracellular acidification thus supporting cancer invasiveness and progression [336].

Similarly, TCA cycle-related enzymes have been found deregulated in breast cancer. Recent studies showed a reduced expression of the PDH complex in luminal subtypes. As described above, PDH catalyzes the oxidative decarboxylation of pyruvate into acetyl-CoA coordinating the flow of metabolites from glycolysis to TCA cycle. Its decreased expression is related to an impaired mitochondrial oxidation and to the promotion of extracellular acidification and cell proliferation [337]. Enhanced succinate and fumarate levels have been found in TNBC compared to ER+ tumors, suggesting the potential increase of TCA cycle activity in hormone-

independent tumors [338]. Excessive levels of fumarate can be caused by impairment of fumarate hydratase (FH) activity or somatic *FH* mutation, the enzyme that catalyzes the reversible hydration/dehydration of fumarate into malate, and have been reported in basal-like tumors [334].

Finally, breast cancer frequently develops a lipogenic phenotype and shows alterations in genes involved in lipid biosynthesis. Unlike the majority of normal mammary cells that solely rely on dietary lipids or use lipids synthesized by the liver, breast cancer cells almost universally exhibit a shift towards an increased lipogenesis. The aberrant *de novo* FA and cholesterol biosynthesis exerts a pivotal role in providing a constant supply of building blocks for membrane synthesis, signaling molecules, and energetic substrates for tumor cells adapting to unfavorable microenvironmental conditions (e.g., limited nutrient availability or drug-induced cytotoxicity) [339].

Breast cancer subtypes also differ in their intracellular FA utilization. Interestingly, it has been recently demonstrated that TNBC preferentially accumulate palmitate into storage organelles known as lipid droplets (LD) when compared to luminal cancer cells, which differently shunt palmitate into FA oxidation to produce energy [340]. The HER2+ subtype differs from TNBC in the expression levels of genes encoding for enzymes involved in FA biosynthesis such as ACLY (ATP-citrate lyase) and FASN (fatty acid synthase). Indeed, TNBC display lower expression of these enzymes suggesting that *de novo* lipogenesis is mainly exploited by the HER2+ subtype [341].

In addition, breast cancer subtypes also differ in the intracellular levels of lipid derived metabolites. Indeed, the primary metabolite of cholesterol, 27-hydroxycholesterol (27-HC), acts as a selective ER modulator resulting in an extensive ER recruitment to target genes thus contributing to proliferation and aggressive features in the ER+ subtype [342].

The role of tumor microenvironment in changing the metabolism of breast tumor cells has been extensively investigated. Hypoxia leads to the stabilization of HIF1-α which in turn promotes the transcription of genes involved in the glycolytic pathway while impairing the activity of enzymes engaged in the TCA cycle [277, 278]. The extracellular acidification stimulates the proteolytic activity of metalloproteases and the subsequent extracellular matrix remodeling which facilitate tumor invasion and metastasis formation [343]. The enhanced lactate production also causes the secretion of VEGF by tumor associated stromal cells leading to extended angiogenesis [344]. Moreover, cancer cells need the detachment from the extracellular matrix (ECM) in order to metastasize. This process can cause changes in metabolic pathways such as reduced glucose uptake, PPP flux, and cellular ATP levels while increasing the ROS production.

In addition to remodeling their metabolic program, breast cancer cells can influence the metabolism of the surrounding stromal cells such as cancer associated fibroblasts (CAF). Co-culture experiments have demonstrated that ER+ breast cancer cells induce oxidative stress and HIF-1α expression in adjacent fibroblasts, resulting in the rewiring of their metabolism

towards mitophagy and improved aerobic glycolysis. In turn, the lactate released from the glycolytic CAF is then utilized by breast tumor cells to fuel their reprogrammed oxidative phenotype in a phenomenon known as the “reverse Warburg effect” [345, 346].
In summary, understanding the metabolic alterations that characterize different types of breast cancer is crucial to identify possible prognostic and predictive metabolic markers and define subsets of patients that can benefit from metabolic drugs currently used in the preclinical setting.

6.1 Deregulated metabolism and therapy resistance in breast cancer

Emerging evidence highlight a strong correlation between breast cancer metabolic reprogramming and resistance to anti-tumoral therapies, suggesting that metabolic alterations could represent a promising target to improve the efficacy of conventional treatments. Several deregulated metabolic pathways in breast cancer such as increased glycolysis, enhanced glutamine utilization, and improved FA metabolism have been linked to therapy resistance [347, 348].
Particularly, it has been shown that the ER+ subtype may evade ET by switching towards alternative metabolic processes. ER+ tamoxifen resistant breast cancer cells are characterized by HIF1-α stabilization which sustains glycolysis through the promotion of HK2 and PDK1 expression and activity via the PI3K/AKT/mTOR signaling pathway thus resulting in enhanced aerobic glycolysis and Warburg-like metabolism. Glycolysis targeting restores tamoxifen sensitivity in drug resistant cells, representing a potential therapeutic strategy for treating tamoxifen resistant breast cancer patients [349].
The aggressive features of ER+ metastatic breast cancer harboring mutations in the LBD domain of ER could be supported by rewired metabolic pathways. In particular, breast cancer cells expressing a mutated receptor show a different metabolic profile than those with wild-type *ESR1*. These cells display a glucose-independent tumorigenic activity, elevated TCA cycle and increased glutamine metabolism, correlated to an adverse clinical outcome [350].
More recently, we have demonstrated a strong correlation between increased levels of miR-23b-3p expression, downregulated expression of the basic and neutral amino acid transporter SLC6A14 (solute carrier family 6 member 14), and ET resistance in ER+ breast cancer. Interestingly, this dysregulation results in impaired amino acid metabolism supported first by the activation of autophagy and second by the selective import of aspartate and glutamate mediated by SLC1A2 (solute carrier family 1 member 2), sustaining anabolic and catabolic processes and promoting the metabolic adaption that supports ET resistance [[351] (**Figure 12**). More details on this work will be provided in Chapter III.

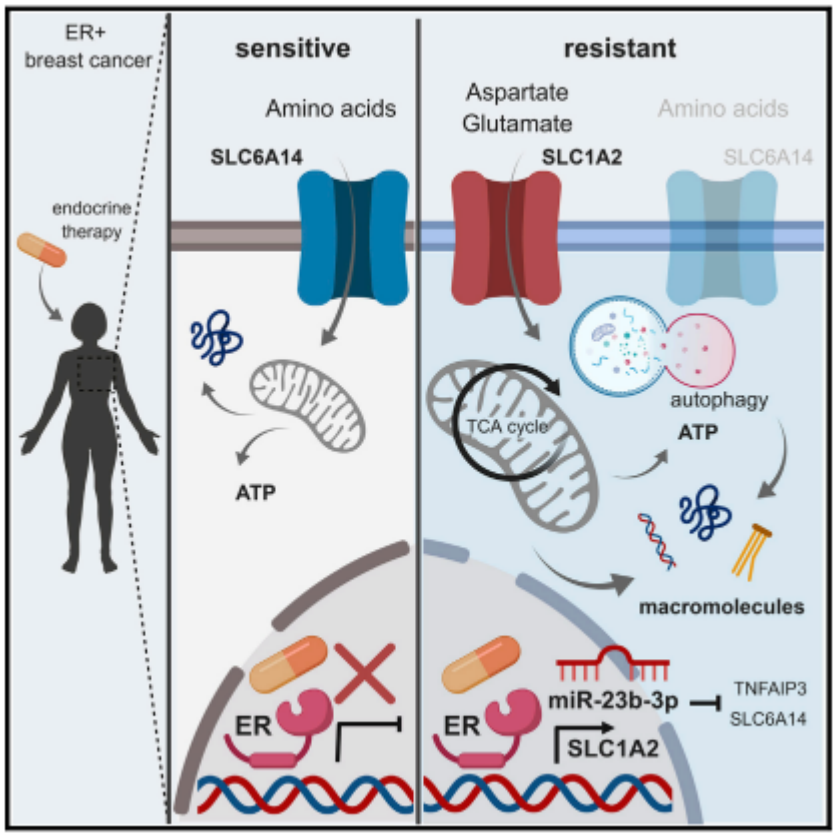

Figure 12. Reprogramming of amino acid transporters to support aspartate and glutamate dependency and sustain ET resistance in ER+ breast cancer.

Our laboratory has also previously identified the upregulation of miR-155 in ER+ breast cancer as a driver of AI resistance. Indeed, the miR-155/HK2 axis is an important regulator of the tumor metabolic plasticity that characterizes AI resistant cells which can adapt to metabolic stress by switching *ad hoc* between OXPHOS and glycolysis when one of these pathways is impaired [352] (**Figure 13**).

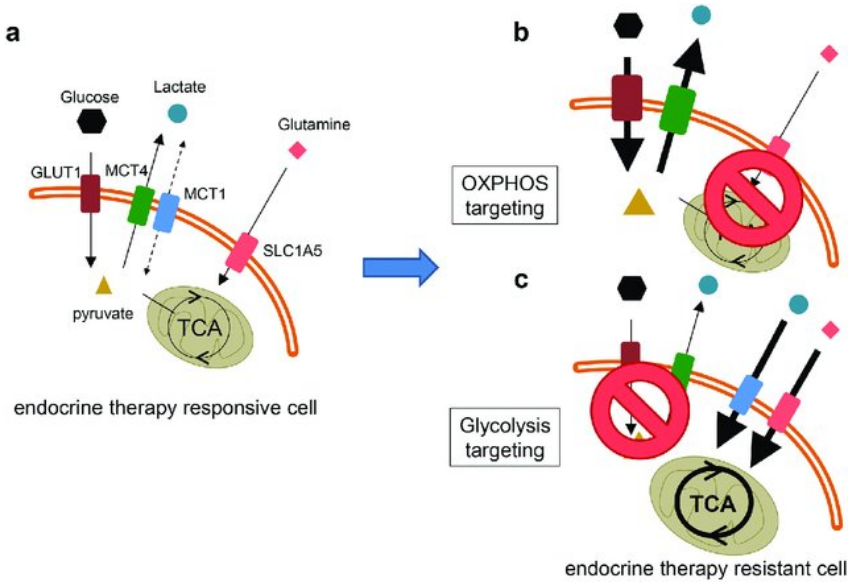

Figure 13. Metabolic plasticity in ER+ breast cancer resistant to ET (taken from [353]).

c-Myc-mediated glutamine metabolism has also been found to be associated with AI resistance in breast cancer. The bidirectional crosstalk between ER and HER2 in AI resistant breast cancer cells promotes the upregulation of c-Myc which in turn allows glutamine uptake through the cognate transporter SLC1A5, thus sustaining glutamine metabolism. The inhibition of c-Myc and SLC1A5 impairs the proliferation of AI resistant cells [354].

Interestingly, enhanced lipogenesis, increased lipid content, and lipid-dependent catabolism can sustain the therapy desensitization and the emergence of a resistant phenotype in breast cancer cells. It has been recently reported that AI resistant breast cancers activate a series of transcription factors, that play a key role in the induction of lipogenesis (i.e., sterol regulatory element-binding transcription factor, SREBP-1 and SREBP-2), and enzymes such as FASN and are more sensitive to SREBPs targeting [355]. In addition, a stable epigenetic activation of the cholesterol biosynthetic pathway that culminates in enhanced intracellular levels of the primary metabolite of cholesterol, 27-HC, regulates ER-dependent genes and sustains ET resistance and breast cancer aggressiveness [342]. This epigenetic and transcriptomic profile, together with 25-HC and 27-HC oxysterol levels, has prognostic and predictive value for breast cancer patients receiving ET [356]. Among the traits that correlate with metabolic alterations and therapy resistance, it has been recently demonstrated that altered lipid metabolism induces ROS-mediated DNA damage, a feature of cells able to survive the therapeutic intervention in preclinical models of breast cancer and responsible for tumor progression from minimal residual disease towards relapse in neo-adjuvant treated breast cancer patients. Crucially, FA biosynthesis perturbation using the FASN inhibitor C75 significantly reduces the oxidative stress and attenuates breast cancer recurrence [357].

Some of the described resistance mechanisms could be overcome by the addiction of CDK4/6 inhibitors to anti-estrogen treatment in ER+ metastatic breast cancer. Nevertheless, despite the clinical advances of a combinatorial therapy using ET plus CDK4/6 inhibitors, numerous studies have reported an emerging metabolic adaption also as determinant of resistance to CDK4/6 inhibitors. For example, we have recently demonstrated that ER+/HER2+ and ER+/HER2− breast cancer cells rely on aerobic glycolysis differently when mimicking a sensitive or a resistant clinical scenario (**Figure 14**). Specifically, targeting glucose metabolism can re-sensitize ER+/HER2+ resistant cells to palbociclib and significantly potentiates its anti-tumoral effect in ER+/HER2− sensitive subset [225]. More details will be revealed in the current thesis (Chapter IV).

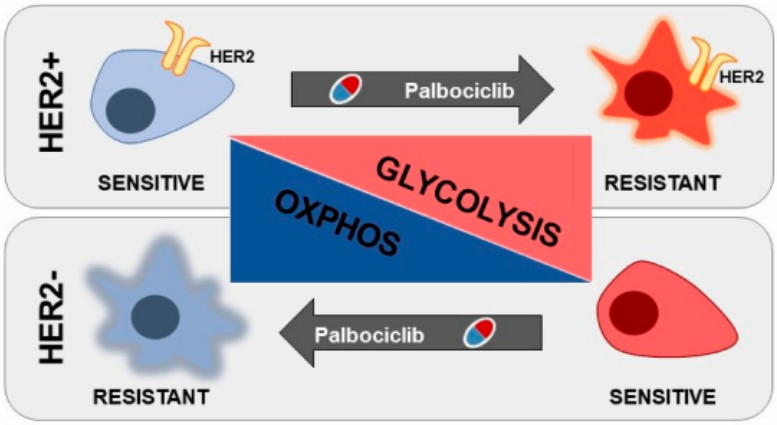

Figure 14. Graphical representation of central carbon metabolic reprogramming in palbociclib resistant ER+ breast cancer.

6.2 Metabolic targeting in breast cancer

As described above, the aberrant metabolic reprogramming occurring in breast cancer cells is linked to their plasticity in adapting to anti-tumoral therapies. Targeting the metabolic pathways abnormally activated in breast cancer could be a promising strategy to improve the efficacy of the standard treatments and to overcome resistance to chemotherapy, ET, and HER2-targeted therapy. The principal metabolic pathways targetable by antimetabolic drugs are: (i) uptake of the main nutrients that cells rely on, (ii) glycolysis and Warburg metabolism, (iii) TCA cycle and OXHPHOS, (iv) glutaminolysis, and (v) FA metabolism (**Figure 15**). To date, encouraging results have been obtained by the combination of metabolic inhibitors and chemotherapeutic regimens in overcoming therapy resistance in different preclinical models of liquid and solid cancers [347, 358-360]. Unfortunately, the transition from the preclinical to the clinical setting is yet to be completed.

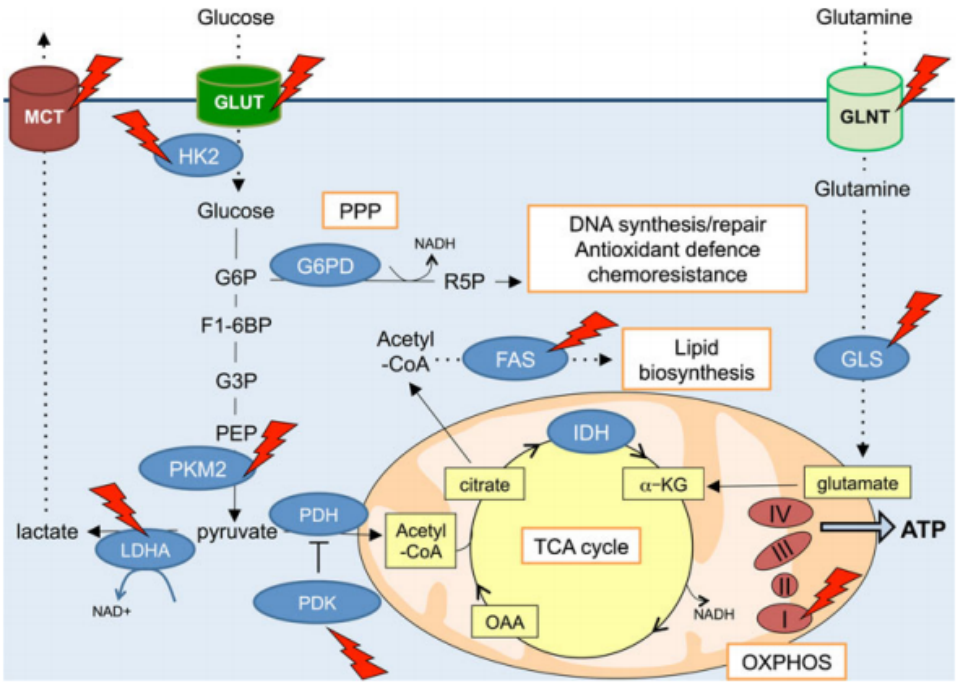

Figure 15. Metabolic targeting in breast cancer (taken from [361]).

Based on the differential metabolic signatures among the molecular breast cancer subtypes, targeting glycolysis might represent a therapeutic strategy more efficient in HER2-enriched and basal-like tumors compared to the luminal subset. 2-deoxyglucose (2-DG) is a glucose analogue that competitively binds to HK2 and inhibits glycolysis. 2-DG enters cell via glucose transporters and is phosphorylated by HK2 but, unlike glucose, it cannot be further metabolized. Thus, 2-DG-6P accumulates into cytoplasm and inhibits glucose catabolism [362]. The increase of HK2 expression has been showed as a prognostic factor in breast cancer and is associated with high rate of proliferation in breast cancer cells [363]. HK2 is additionally inhibited by a series of agents (e.g., 3-bromopyruvate and ionidamide) that have also been clinically investigated. Although glycolysis targeting has no significant effect as monotherapy, HK2 targeting synergizes with trastuzumab in sensitive cells and reverts resistance in models insensitive to the treatment both *in vitro* and *in vivo* [364]. Additional strategies involve the use of small molecule antagonists of 6-phosphofructo-2-kinase/fructose-2,6-biphosphatase 3 enzyme (PFKFB3) which produces fructose-2,6-bisphosphate (F26BP), that is a potent allosteric activator of the glycolytic enzyme PFK1. Constitutive HER2 expression leads to high PFKFB3 levels and increases glucose metabolism; thus, the suppression of PFKFB3 activity reduces the steady-state concentration of F26BP and suppresses PFK1 activity and glucose uptake. Therefore, PFKFB3 targeting may be an effective treatment in combination with trastuzumab in sensitive breast cancer and may re-sensitize resistant tumor to anti-HER2 therapy [365].

The inhibition of lactic fermentation is effective in reducing the tumor microenvironment acidification and diverting pyruvate into mitochondria. Indeed, LDH knockdown potentiates the

oxidative respiration, decreases proliferation, and affects tumorigenicity in breast cancer cells [232]. Moreover, LDHA blockade by oxamate or FX11 re-sensitizes breast cancer paclitaxel and trastuzumab resistant cells to the initial therapy by promoting apoptosis [366, 367]. Dichloroacetate (DCA) is a PDK inhibitor responsible for a metabolic shift from glycolysis to OXPHOS by promoting the conversion of pyruvate into acetyl-CoA and has been suggested in combination strategies for the treatment of metastatic breast cancer [368]. Besides the inhibition of glycolytic enzymes, impairing GLUT1 activity using WZB117 has shown synergistic inhibitory effect in breast cancer cells [369].

Mitochondrial respiration and OXPHOS have been also indicated as adaptive mechanisms driving aggressiveness in tumors including breast cancer [370-372]. Metformin is an antidiabetic clinically approved drug that has also been investigated as anti-tumoral therapy due to its ability in impairing OXPHOS by targeting complex I in mitochondrial ETC and has been shown to exert anti-cancer activity also in breast cancer [373] and synergize with standard chemotherapy in reverting drug resistance [374]. Furthermore, metformin reveals high selectivity in targeting breast cancer stem cells characterized by an enhanced mitochondrial metabolism [375].

In addition to glucose metabolism, glutamine dependency is another altered pathway to escape drug treatment. Therefore, inhibition of glutamine uptake and metabolism through the selective targeting of membrane transporters and glutaminolysis may represent a potential pharmacological strategy in breast cancer. Two novel glutaminase inhibitors CB-839 and CB-968 have shown to enhance chemotherapy sensitivity in combination with paclitaxel or doxorubicin in TNBC cell lines by activating apoptosis and suppressing invasiveness [310, 341, 376].

Aberrant lipid metabolism has also emerged as a potential metabolic vulnerability that could be exploited for altering the response to anti-cancer therapy and reverting drug resistance. The inhibition of FASN re-sensitizes to trastuzumab and synergizes with paclitaxel and docetaxel in HER2+ resistant breast cancers [377-383]. An array of FASN inhibitors is now available (e.g., cerulenin, C75, TVB-2640, orlistat), but most of them are associated with poor pharmacokinetics, selectivity issues, and toxicity. However, TVB-2640 inhibitor, which showed promising results in the preclinical setting, is currently assessed as adjuvant therapy in a phase II clinical trial in combination with chemotherapy or trastuzumab in metastatic HER2+ breast cancer patients that have already experienced resistance to taxane or trastuzumab [ClinicalTrials.gov; https://clinicaltrials.gov/ct2/show/NCT03179904].

Moreover, the contribution of exogenous FA to anti-cancer therapy response has been demonstrated in HER2+ breast cancers, which normally are dependent on *de novo* FA biosynthesis due to the induction of FASN mediated by HER2 downstream signaling activation. HER2+ breast cancer cells that are resistant to the EGFR/HER2 inhibitor lapatinib upregulate the FA transporter CD36 to maximize exogenous FA uptake and lipid storage. CD36-mediated

FA uptake may be targeted using an anti-CD36 antibody or the sulfosuccinimidyl oleate inhibitor that re-sensitize anti-HER2 therapy resistant breast cancers to the initial therapy [384].

The increased lipid uptake of cancer cells may be exploited to fuel FA oxidation and therefore satisfy cancer cell energetic demands. Therefore, impairing either the entry or the subsequent oxidative catabolism of FA could impact on therapy response and resistance. FA oxidation has been linked to radio and chemoresistance in breast cancer. An increase in CPT1A and CPT2 expression with consequent elevated FA oxidation occurs in radioresistant breast cancer stem cells (CSC), which are responsible for disease relapse [385]. Elevated FA oxidation is associated with increased activation of pro-survival ERK1/2 pathway, revealing a potential crosstalk between metabolic alteration and proliferation signaling. FA oxidation inhibition by etomoxir treatment impairs ERK1/2 activation and re-sensitizes radioresistant breast CSC to radiation therapy [386]. Moreover, combinatorial treatment with paclitaxel and the FA oxidation inhibitor perhexiline re-sensitizes resistant TNBC cells to chemotherapy [387].

Finally, in light of this scenario, the emergence of resistance contributes to treatment failure and precludes complete remission. Given all these evidence, therapeutic strategies should be adjusted to prevent recurrence and combinatorial therapies may provide an effective solution that both limits cancer cell progression and suppresses tumor metabolic reprogramming associated aggressiveness.

Chapter II. Materials and Methods

1. Materials

- Unless specified, all reagents used for cell culture were purchased from Euroclone Group, Invitrogen, and Sigma-Aldrich.
- Solutions and equipment for protein analysis, including materials for SDS-PAGE (Sodium Dodecyl Sulphate-PolyAcrylamide Gel Electrophoresis) and immunoblotting were purchased from Biorad.
- Protease and phosphatase inhibitors were from Sigma-Aldrich.
- BCA reagent and Bradford reagent for protein dosage were from Sigma-Aldrich and Biorad, respectively.
- Protein A/G PLUS-agarose was purchased from Santa Cruz Biotechnologies.
- Chemiluminescence revelation kits were from GE Health Care and Biorad.
- Transwells for migration and invasion assays were from Costar (Euroclone Group). The Diff-Quick staining was purchased from BIOMAP SNC.
- All radiolabeled molecules were purchased from PerkinElmer.
- Reagents for RNA extraction, cDNA synthesis, and RT-PCR were from Qiagen, Applied Biosystem, and Biorad.
- Seahorse XFe96 kits were from Agilent Technology.

1.1 Cell lines

MCF7, ZR75-1, and HCC1428 human female breast cancer cells were purchased from ATCC (American Type Culture Collection) and maintained in phenol red-free RPMI 1640 medium (Gibco) containing 10% fetal bovine serum (FBS, Euroclone), 2 mM glutamine (Sigma), and 1 nmol/L E2 (Sigma). For functional assays, MCF7 parental cells were deprived from E2 for 72 hours (h) to obtained MCF7-E2 and mimic the acute treatment with an AI. LTED (long-term estrogen deprived) cells were obtained by culturing parental cells in a medium deprived from E2 for at least 20 weeks, to mimic the chronic treatment and the AI resistance. LTED derivatives were cultured in RPMI1640 medium without phenol red, supplemented with 10% dextran charcoal stripped FBS (DCC, Hyclone) and 2 mM glutamine (DCC medium). Tamoxifen (TAMR) and fulvestrant (FULVR) resistant cells were obtained by culturing MCF7 parental cells in DCC medium with increasing concentrations of the drugs for at least 12 weeks and represent cellular models of tamoxifen and fulvestrant resistance, respectively. MCF7 TAMR and MCF7 FULVR cells were cultured in DCC medium and treated with 1 mmol/L 4-OH tamoxifen (Sigma) or 100 nmol/L fulvestrant (Sigma), respectively.

ZR75-1 and T47D (ER+/HER2−) human female breast cancer cell lines were kindly provided by Dr Livia Malorni (CNR, Avellino); ER+/HER2+ MDA-MB-361 cells were purchased from Sigma-Aldrich and BT474 cells from Interlab Cell Line Collection. All these cell lines were maintained in Dulbecco's Modified Eagle Medium (DMEM, Euroclone), supplemented with 10% FBS, 2 mM glutamine, and 1% penicillin/streptomycin (Sigma). The palbociclib resistant derivatives (PDR cells) were obtained by culturing parental cells with increasing doses of the drug for around 6-9 months and cultured in the same condition in the presence of the final concentration of 1 μM palbociclib (Pfizer). To evaluate cell viability under either glucose deprivation or galactose-containing medium, the cells were cultured in "deprived" DMEM 1X (Gibco), supplemented with or without 25 mM glucose (Sigma), in the presence of 10% FBS, 2 mM glutamine, and 110 mg/L pyruvate (Sigma). 2-deoxyglucose (2-DG, Sigma) and galactose (Sigma) were supplemented to the medium at the concentration of 5 mM and 25 mM, respectively.
Cells were short tandem repeat tested, amplified, stocked, routinely subjected to mycoplasma test and, once thawed, were kept in culture for a maximum of 20 passages.

1.2 Mouse models and care

5- to 6-week-old female BALB/c mice were purchased from Charles River Laboratories and used for lung retention assays. Animal work was conducted under the Project licenses 1002/2017-PR, approved by the Ministero della Salute. All animals were monitored by dedicated scientists from the *Centro Stabulazione Animali da Laboratorio* (CESAL) for symptoms of illness. Mice were housed under sterile conditions (five or less animals per cage) with access to food and water. For patient derived xenografts (PDX), 8- to 10-week-old NSG female mice were used and experiments were performed at the University of Manchester. Serial passaging of the PDX was performed by implanting subcutaneously small fragments of the tumor into the dorsal flanks of NSG mice. HBCx34 breast cancer estrogen-dependent PDX were treated with 8 mg/mL of E2 in drinking water at all times. HBCx34 TAMR PDX were treated for the complete duration of the experiment with tamoxifen (10 mg/kg/day, oral gavage). Experiments were performed using PDX tumors between passages 5 and 8. Animal weight and tumor size were measured twice a week. Tumor fragments were snap frozen and utilized for either RNA extraction and qRT-PCR (Quantitative Real-Time Polymerase Chain Reaction analysis) or GC-MS (Gas Chromatography-Mass Spectrometry).

1.3 Common use solutions

- PBS (Phosphate Buffered Saline): 0.27 g/L di KH_2PO_4, 0.2 g/L KCl, 8.01 g/L NaCl, 1.78 g/L NaH_2PO_4 pH 7.4.

- RIPA lysis buffer: 50 mM Tris-HCl pH 7.5, 150 mM NaCl, 1% Nonidet P-40, 2 mM EGTA, 100 mM sodium orthovanadate, 100 mM NaF.
- Lysis buffer: Sample Buffer 1X (SB1X).
- SDS−PAGE 4X Sample Buffer: 40% glycerol, 240 mM Tris-HCl pH 6.8, 8% SDS, 0.04% bromophenol blue, 5% β-mercaptoethanol.
- SDS-PAGE 1X running buffer: 25 mM Tris, 192 mM glycine, 0.1% (W/V) SDS, pH 8.3.
- SDS-PAGE 1X blotting buffer: 25 mM Tris, 192 mM glycine, 10% methanol, pH 8.3.
- Blocking solution: non-fat dry milk 2%, tween 0.05% in PBS.
- Washing solution: tween 0.1% in PBS 10X (T-PBS).

1.4 Drugs, compounds, and reagents

- E2: dissolved in 100% ethanol at 1 μM, stored at -20°C, purchased from Sigma.
- 4-OH tamoxifen: (hereafter simply tamoxifen) dissolved in 100% ethanol at 10 mM, stored at -20°C, purchased from Sigma.
- ICI-182,780 (fulvestrant): dissolved in DMSO at 10 mM, stored at -20°C, purchased from Tocris Bioscience.
- Palbociclib (PD): dissolved in DMSO (dimethyl sulfoxide) at 10 mM, stored at -20°C, purchased from Pfizer.
- Glucose: stored at room temperature, purchased from Sigma.
- 2-DG: dissolved in PBS at 100 mg/mL, stored at +4°C, purchased form Sigma.
- MTT (3-(4,5-dimethylthiazol-2-yl)-2,5-diphenyltetrazolium bromide): dissolved in culture medium at 5 mg/mL, stored at 4°C.
- Chloroquine diphosphate salt (hereafter referred to as CQ): dissolved in H_20 at 25 or 50 μM, stored at -20°C, and purchased from Sigma.

1.5 Antibodies

Antibody	Application	Dilution	Use	Source	Manifacturer
SLC6A14	WB	1:1.000	O/n 4°C	Rabbit	Abcam
SLC1A2	WB	1:1.000	O/n 4°C	Mouse	Santa Cruz Biotechnologies
LC3	WB	1:500	O/n 4°C	Rabbit	Invitrogen
Beclin-1	WB	1:1.000	O/n 4°C	Rabbit	Thermo Fisher
Beclin-1	IP	4 μg/250 μL	O/n 4°C	Rabbit	Santa Cruz Biotechnologies

Ub-K63	IP	1:1.000	O/n 4°C	Mouse	eBioscience
GLUT1	WB	1:1.000	O/n 4°C	Rabbit	Cell Signaling
HK2	WB	1:1.000	O/n 4°C	Rabbit	Cell Signaling
MCT1	WB	1:500	O/n 4°C	Rabbit	Santa Cruz Biotechnologies
MCT4	WB	1:500	O/n 4°C	Rabbit	Santa Cruz Biotechnologies
Tubulin	WB	1:25.000	1 h room temperature	Mouse	Sigma

2. Methods

2.1 General culture conditions

Cell lines were grown under 5% CO_2 incubation at 37°C in their corresponding culture medium. For cell passaging, growth medium was removed, and the cells were washed with PBS and incubated with a covering volume of trypsin for 1-2 minutes (min). When cells were detached, medium was added to neutralize trypsin's effect and cells were seeded into a new flask.

2.1.1 Long-term cell frozen storage

Cells were detached using trypsin, resuspended into their cell culture medium, and pelleted by centrifugation at 1.000 rpm (rotation per minute) for 5 min. Then, pellet was resuspended in 1 mL of cell freezing medium (90% FBS/DCC and 10% DMSO) and cells transferred into specific freezing vials, stored in polystyrene insulated boxes at -80°C for at least 48 h and subsequently in liquid nitrogen for long time. For the thawing procedure, cells were moved into a new flask and resuspended with fresh cell culture medium. The following day, medium was replaced to completely remove DMSO.

2.2 Immunofluorescence

Glass coverslip (Thermo Fisher)-plated cells were fixed with 4% formaldehyde for 1 h, permeabilized with 0.1% triton in PBS, and then incubated with the primary antibody diluted 1/400 in blocking solution (1% BSA and 2% serum in PBS), overnight at 4°C. Secondary antibody conjugated with Alexa Fluor 488 or 633 (Life Technologies) was diluted in blocking solution 1/1.000 and incubated for 1 h at room temperature. All fluorescence samples were examined using a microscope TCS SP5 (Leica) with lasers exciting at 488, 543, and 633 nm.

Multicolor images were collected using the Leica LAS-AF image acquisition software. The quantification was performed using FiJi: an outline was drawn around each cell and spots were counted in at least 50 cells derived from three representative 63x images from 3 independent experiments.

2.3 Protein manipulation

Protein extraction: cells were washed twice in cold PBS and then lysed with SB 1X or RIPA buffer supplemented with protease and phosphatase inhibitors (1/100). Protein lysates were collected, kept in ice, and centrifuged at 12.000 rpm for 10 min. After centrifugation, the supernatant was collected, and total proteins were quantified with either BCA (bicinchoninic acid) protein assay or Bradford assay.

Protein quantification: The BCA protein assay is based on the notion that proteins can reduce Cu^{+2} to Cu^{+1} in an alkaline solution containing BCA resulting in a purple color formation. The absorbance of the BCA/copper complex at 562 nm is directly proportional to the protein concentration. To prepare BCA solution, we combined 50 parts of A solution with 1 part of B solution. In cuvettes for spectrophotometer, we added 45 uL of water (50 uL for the blank), 5 uL of each protein lysate sample, and 950 uL of BCA solution. After 30 min of incubation at 37°C, all the samples and the blank were read by the spectrophotometer at a wavelength of 562 nm.
Protein quantification was also evaluated with Coomassie Brilliant Blue (Bradford protein assay), which binds to basic and aromatic amino acidic residues (especially arginine), leading to a maximum absorption at 595 nm wavelength. Thus, Coomassie Brilliant Blue intensity is positively correlated to the protein concentration. The Bradford reagent is prepared diluting 1/5 of the starting solution Coomassie Brilliant Blue in 4/5 of deionized water (dH_2O). For the quantification, 5 µL of each sample, opportunely diluted in 45 µL of water, were added to 950 µL of the working solution. After 5 min incubation, the absorbance of each sample was evaluated at a wavelength of 595 nm.
To generate the standard curve, we used Bovine Serum Albumin (BSA), diluting BSA 2 mg/mL concentrated in dH_2O to obtain BSA concentrations from 2 µg/mL to 15 µg/mL. Thus, from the values obtained from the standard curve, it is possible to create a curve of the absorbance in function of the concentration; consequently, interpolating absorbance values to the standard curve, it is possible to calculate the final protein concentration of the samples of interest. Correlation between absorbance and concentration is expressed by Lambert-Beer law: $A=\varepsilon dc$, where ε represents the molar extinction coefficient, d represents the path length, and c the sample concentration.

SDS-PAGE: it is a technique used for protein separation thanks to their ability to move within an electric current, which is a function of the length of their polypeptide chains or of their molecular weight. This is achieved by adding SDS detergent to remove secondary and tertiary protein structures and to maintain the proteins as polypeptide chains. SDS-PAGE samples were boiled for 5 min in SB 4x plus β-mercaptoethanol, which leads to disulphuric bond reduction and destabilization of protein tertiary structure. In addition, SB was supplemented with bromophenol blue, an ionizing colored-tracking solution, and glycerol which increases sample density and promotes its stratification at the bottom of the loading well. The gels used were precast SDS-PAGE gels (Biorad), with a range of acrylamide concentration from 4% to 20%, required to better stratify the samples before entering the separating gel. 20-40 µg of total proteins were loaded into the wells of the stacking gel and an electric field was applied across the gel, allowing the negatively charged proteins to migrate across the gel towards the positive electrode (anode). Protein relative molecular mass was evaluated by comparison with protein ladder standard molecular weights, separated into the same gel. Running was performed at 100-150 V for almost 1 h.

2.3.1 Immunoblotting

After running, protein samples were transferred from the gel to a nitrocellulose membrane (blotting) by Trans-Blot Turbo Transfer Pack (Biorad) to make the proteins accessible for the antibody detection. The proteins embedded into the gel are transferred to the membrane maintaining the organization that they have within the gel. Protein transfer was carried out at 25 V and 2.5 A for either 7 min (for proteins with low molecular weight) or 10 min (for proteins with high molecular weight). After blotting, the membrane was incubated for 1 h in the blocking solution (non-fat dry milk 2%, tween 0.05% in PBS) at room temperature and then overnight in slow agitation at 4°C in a blocking solution with the specific primary antibody. The following day, the membrane was washed three times with a solution of T-PBS and then incubated with the horseradish peroxidase (HRP)-conjugated secondary antibody for 1 h at room temperature and finally washed again for three times with T-PBS. In the chemiluminescence reaction, HRP catalyzes the oxidation of luminol into a reagent which emits light when it decays. Since the HRP is complexed with the secondary antibody specific for the protein of interest on the membrane, amount and location of the emission light are directly correlated with those of the protein of interest. Chemiluminescent protein revelation was carried out with ECL Western Blotting reagents (Biorad) at the Amersham Imager 600. Exposure was repeated varying the time as needed for the optimal detection.

The antibodies used for the first part of the thesis were SLC1A2 (Santa Cruz Biotechnology), SLC6A14 (Abcam), beclin-1 (Invitrogen), LC3 (Invitrogen), ubiquitin-K63 (Thermo Fisher), and

tubulin (Sigma). The antibodies used in the second part of the work were GLUT1 and HKII (Cell Signaling), MCT1 and MCT4 (Santa Cruz Biotechnologies), and tubulin (Sigma).

2.3.2 Immunoprecipitation

For the immunoprecipitation of beclin-1, MCF7 parental, MCF7 LTED, MCF7 TAMR, and MCF7 FULVR cells were lysed with c-RIPA (RIPA with the addition of deoxycholate 5% and SDS 1%) lysis buffer supplemented with protease and phosphatase inhibitors. The cells were lysed as previously described and then, after centrifugation, the supernatant was incubated with 4 µg/250 µL of anti-beclin-1 antibody overnight at 4°C. Cell lysates were immunoprecipitated with 20 µL of protein A/G PLUS agarose beads (Santa Cruz Biotechnology) at 4°C for 1-4 h in agitation. The precipitates were washed three times with c-RIPA, resuspended in 20 µL of SB, boiled, and subjected to immunoblotting analysis.

2.4 Protein *de novo* synthesis assay

To evaluate protein *de novo* synthesis percentage in ET resistant cells compared to parental cells, 30,000 cells were seeded per well in a 96-well clear bottom black plate (Corning). The following day, the culture medium was removed, and cells were incubated for 30 min in fresh culture medium containing O-Propargyl-Puromycin (OPP) with or without 50 µg/mL cycloheximide. OPP incorporates into the C-terminal of translating polypeptide chains, thereby blocking the translation. Cells were then processed for the detection of protein synthesis according to the protocol of Cayman Chemicals Protein Synthesis assay (Cayman Chemicals).

2.5 RNA manipulation

Total RNA was extracted from cultured cells, grown as monolayer, using RNeasy Mini Kit (Qiagen). RNA concentration and quality of the samples were determined by measuring the UV absorbance at 260 nm and 280 nm on Nanodrop 1000 (Thermo Scientific), and 500 ng of total RNA were reverse transcribed to cDNA using QuantiTect cDNA reverse transcription kit (Qiagen), according to manufacturer's instructions.
Moreover, total RNA, including small RNA, was extracted using miRNeasy Mini Kit (Qiagen), quantified, and 10 ng were reverse transcribed using Taqman MicroRNA Reverse Transcription Kit (Applied Biosystems) for miRNA analysis, according to manufacturer's instructions.

2.6 Quantitative Real-Time Polymerase Chain Reaction

qRT-PCR is a method by which the amount of the PCR product can be determined in real-time, and is useful for investigating gene expression using a fluorescent reporter whose signal strength is directly proportional to the number of amplified DNA molecules. qRT-PCR was done using the 7500 Fast Real-Time PCR system (Applied Biosystems) or the CFX96 Touch Real-Time PCR Detection System (Biorad), employing Taqman gene/miRNA assays (Applied Biosystems).

The probes used in the first part of the work are: SLC6A14 (Hs00924564_m1), SLC1A2 (Hs01102423_m1), and endogenous controls GAPDH (Hs02786624_g1) and ACTB (Hs99999903_m1)) for mRNA analysis. For miRNA assay, the probes used are miR-23b-3p (ID:000400), and endogenous controls RNU48 (ID:001006) and U6 (ID:001973). TNFAIP3 (HsaCID0012648) and beclin-1 (HsaCID0016032) mRNA expression analysis was performed using SYBR green dye precast primers (Biorad) and normalized on the results obtained using GAPDH (HsaCED0038674) as control. The relative quantity was determined using $\Delta\Delta$Ct, according to the manufacturer's instructions (Applied Biosystems).

The probes used in the second part of the thesis are HKII (Hs0060686_m1) and GLUT1 (Hs00892681_m1). Data were normalized on GAPDH (Hs02786624_g1) and TBP (Hs00427620_m1). The relative quantity was defined using $\Delta\Delta$Ct by the CFX Maestro software (Biorad).

2.7 Cell viability and survival assays

2.7.1 Crystal violet assay

Crystal violet (CV) is a triphenylmethane dye (4-[(4-dimethylaminophenyl)-phenylmethyl]-N, N-dimethylaniline, Sigma), also known as Gentian violet, which allows the DNA quantification that is proportional to the cell number. Breast cancer sensitive and resistant cells were plated in 24- or 12-well plates in either standard conditions or experimental conditions (see Figure legends) such as RNA interfering, drug administration, glycolysis impairment or autophagy targeting. 3 or 5 days post seeding and after the removal of the cell culture medium, cells were fixed with 4% formaldehyde solution at room temperature for 15 min and then stained with CV solution for 10 min at 37°C. CV solution contains 0.5% CV in dH_2O and 20% methanol. After incubation, CV was removed through aspiration and the cells were washed with PBS and dried overnight. Finally, CV within the adherent cells was solubilized using 2% SDS in slow agitation for 20 min at 37°C. The absorbance is evaluated at 595 nm using the microplate reader and is positively correlated to the CV amount bound to cells. Each measurement was made in triplicate.

2.7.2 MTT assay

Alternatively, cell viability was also assessed by MTT (3-[4,5-dimethylthiazol-2-yl]-2,5-diphenyl tetrazolium bromide, Sigma) assay. The MTT assay is used to measure the cellular metabolic activity as an indicator of cell viability, proliferation, and cytotoxicity. This colorimetric assay is based on the reduction of a yellow tetrazolium salt to a purple formazan by metabolically active cells. Indeed, the viable cells contain NAD(P)H-dependent oxidoreductase enzymes which can reduce MTT to formazan.

Cells were plated in 24- or 12-well culture dishes and subjected to different experimental procedures. Then, living cells were stained with 10 mg/mL MTT dissolved in full medium and incubated at 37°C in a humidified atmosphere incubator containing 5% CO_2 for 2-4 h. Finally, cells were extensively washed with PBS, and the incorporated amount of MTT was resuspended

in DMSO and quantified measuring the absorbance at 550 nm using a microplate reader.

2.8 Colony formation assay

To evaluate clonogenicity of breast cancer cells under stress conditions, 500-1,000 cells were seeded per well in a 6-well plate in either the recommended medium conditions or experimental conditions (e.g., amino acid deprivation). 15 days post seeding, colonies were fixed with 4% formaldehyde and stained with CV solution. Air-dried plates were scanned, and images analyzed using FiJi.

2.9 Transwell motility and invasion assay

Transwell system, equipped with 8 µm pore polyvinylpyrrolidone-free polycarbonate filters (Corning), was used. For the invasion assay, the upper side of the porous filter was coated with 50 µg/cm^2 of reconstituted standard formulation Matrigel (BD Biosciences) dissolved in sterile water and incubated over night at room temperature. The following day, cells (previously serum-starved for 6 h) were plated into the upper compartment of the transwell (100,000 cells in 200 µL of serum-free medium), placed into 24-well culture plates containing 500 µL of complete growth medium per well, and allowed to migrate or invade overnight toward the complete medium. Finally, non-invading cells were mechanically removed using cotton swabs from the upper chamber, and the air-dried membrane was stained with Diff-Quick Solutions (BD Biosciences) and imaged. Chemotaxis was evaluated by counting the cells migrated to the lower surface of the filters (six randomly chosen fields).

2.10 RNAi transfection

350-500,000 cells were plated in 6-well culture dishes to reach a 70% of confluence the following day when cells were transfected accordingly to manufacturer's instructions using Lipofectamine RNAiMAX Reagent (Thermo Fisher Scientific) and Opti-MEM (Gibco). Cells were transfected with 15 nmol/L anti-miR-23b-3p (Ambion), with 45 nmol/L siSLC1A2 (Sigma), or 50 nmol/L siRNA targeting HKII (Sigma) and respective negative controls (Ambion, Sigma). The functional analyses were performed 3 days after transfection.

2.11 Radioactive assays

2.11.1 Radiolabeled glucose and amino acid uptake

Breast cancer cells were seeded into 12- or 6-well plates in basal culture conditions or treated as described in the Figure legends. Radiolabeled nutrient (e.g., glucose, aspartic acid, glutamic acid, amino acid pool) uptake was evaluated incubating cells in a buffered solution (140 mM NaCl, 20 mM Hepes/Na, 2.5 mM MgSO4, 1 mM CaCl2, and 5 mM KCl, pH 7.4) containing 0.2 µCi/mL [U-^{14}C]-radioactive metabolites (PerkinElmer) for 15 min at 37°C. Cells were subsequently washed with cold PBS and lysed with 0.1 M NaOH. Incorporated radioactive signal was measured by liquid scintillation counting and normalized on protein content.

2.11.2 Incorporation of radiolabeled amino acids into proteins, lipids, and DNA

To analyze the incorporation of radioactive amino acids into proteins, lipids, or DNA, cell culture medium was changed to a deprived DMEM medium (Gibco), in the presence or absence of non-radioactive amino acids, supplemented with 10% DCC, 11 mM glucose, 2 mmol/L glutamine, and 1 µCi ^{14}C-aspartic acid (PerkinElmer) or 1.5 µCi ^{14}C-glutamic acid (PerkinElmer) 24 h prior to the experiment. For radioactive incorporation into proteins, cells were washed with ice cold PBS and resuspended in 20% trichloroacetic acid (TCA), stored in ice for 30 min and centrifuged (10.000 rpm for 10 min at 4°C). Pellet was resuspended in dH_2O, moved into a scintillation vial, and analyzed with the scintillation counter. For radioactive incorporation into lipids, cells were washed three times with ice cold PBS and then lysed with methanol. Then, samples were resuspended firstly in 4 volumes of a $CHCl_3$:MeOH (1:1) solution and secondly in an additional volume of dH_2O. The solution was centrifuged at 1,000 rpm for 5 min at room temperature and the lower phase was collected, moved into a scintillation vial, and counted. For radioactive incorporation into DNA, cells were washed and then lysed with Tris-HCl 50 mM/EDTA 100mM/SDS 0.5%/proteinase K lysis buffer. Samples were supplemented with one

volume of phenol:chloroform:isoamyl alcohol (25:24:1), mixed, and centrifuged (10,000 rpm for 10 min at room temperature). The upper aqueous phase was recovered, resuspended in 1/10 volume of 3 M NH_4OAc and 2 volumes of ethanol, and incubated for 3 h at -80°C. The precipitated DNA was pelleted (10,000 rpm for 10 min at room temperature), washed with 70% ethanol, and let to dry. Finally, the pellet was resuspended in dH_2O, transferred to a scintillation vial, and analyzed with the scintillation counter. All the radioactive signals were normalized on protein content.

2.12 High-Performance Liquid Chromatography

Amino acid extraction was performed immediately before analysis in ice-cold lysis/extraction buffer (methanol/acetonitrile/water, 5/3/2 v/v, Sigma) starting from $2x10^6$ cells/mL. Tubes were first vortexed at 4°C for 30 min and then centrifuged at 4°C, 10,000 g for 10 min. The supernatant was exposed to a precolumn derivatization of amino acids using 4-N,N-dimethylaminoazobenzene-4'-sulfonyl chloride (DABS, Sigma), following the manufacture instructions. DABS-amino acids were detected at visible light wavelengths (436 nm) using a DIONEX P680-UVD170U High-Performance Liquid Chromatography (HPLC) system (Sigma). A reference amino acid spectrum was obtained by titrating a mixture of amino acids of known concentration (Sigma).

2.13 Gas Chromatography-Mass Spectrometry

Cells or snap frozen tissue samples were subjected to extraction using a mixture of $CHCl_3$:MeOH:H_2O (Sigma) (1:1:1), before quenching with ice-cold MeOH:H_2O (1:1) containing norvaline (Sigma), used as internal standard. One volume of chloroform was added, and the samples were vortexed at 4°C for 30 min, centrifuged at 3,000 g for 10 min, and the aqueous phase was collected into a new tube and allowed to evaporate at room temperature. Dried polar metabolites were dissolved in 60 µL of 2% methoxamine hydrochloride (Sigma) in pyridine (Thermo Fisher) and held at 30°C for 1-2 h. After dissolution and reaction, 90 µL N-Trimethylsilyl-N-methyl trifluoroacetamide (MSTFA) + 1% trimethylchlorosilane (TMCS, Sigma) were added and samples were incubated at 37°C for 60 min. Gas chromatographic runs were performed with helium as carrier gas at 0.6 mL/min. The split inlet temperature was set to 250°C and the injection volume at 1 µL. A split ratio of 1:10 was used. The oven temperature ramp was from 60°C to 325°C at 10°C/min. The data acquisition rate was 10 Hz. For the Quadrupole, an EI (electron ionization) source (70 eV) was used, and full-scan spectra (mass range from 50 to 600) were recorded in the positive ion mode. The ion source and transfer line temperatures were set, respectively, at 250°C and 290°C. For the determination of the relative metabolite

abundance, the integrated signal of all ions for each metabolite was normalized on the signal from norvaline and on the cell number. The MassHunter data processing tool (Agilent) was used to obtain a global metabolic profiling. Fihen Metabolomics RTL library (Agilent).

2.14 ^{13}C-tracing experiments using Liquid Chromatography-Mass Spectrometry

MCF7 parental and LTED cells were incubated for 48 h with 0.15 mM [U-^{13}C]-aspartic acid (Cambridge Isotope Laboratories) or 0.13 mM [U-^{13}C]-L-glutamic acid (Sigma). Cells were washed with ice cold 0.9% NaCl solution. The metabolite extraction was performed using 80% methanol. After 5 min of incubation, cells were scraped and collected in a new tube. Following a centrifugation at 20.000 g for 10 min at 4°C, the supernatant was transferred into a new vial for Liquid Chromatography-Mass Spectrometry (LC-MS) analysis. Pellet was used for protein quantification. 5 µL of each sample were loaded into a Dionex UltiMate 3000 LC System (Thermo Scientific Bremen) equipped with a C-18 column coupled to a Q Exactive Orbitrap mass spectrometer (Thermo Scientific) operating in negative ion mode. A step gradient was carried out using solvent A (10 mM TBA and 15 mM acetic acid) and solvent B (100% methanol). The chromatography was stopped at 40 min. The flow was kept constant at 250 µL/min and the column was placed at 25°C throughout the analysis. For the data analyses, we integrated the peak areas using the Thermo XCalibur Quan Browser software (Thermo Scientific).

2.15 Metabolomics data analysis

GC-MS derived chromatograms and spectra were analyzed using MassHunter Qualitative Analysis and then processed using Profinder (Agilent Technologies). Profinder returned 3.624 aligned compounds using the following filters: m/z range (100–1,000 m/z), absolute peak height (>10,000 counts), number of ions required (≥5 ions). Data generated were subjected to Mass Profiler Professional (MPP, Agilent Technologies) and subjected to statistical analysis using Tukey's honest significant difference (HSD)-corrected analysis of variance (ANOVA). Differentially expressed m/z entities were chosen to have an adjusted p-value ≤ 0.05 in the ANOVA test, with a Benjamini and Hochberg correction. This analysis returned 1,953 entities that were then further processed using MPP for the principal component analysis (PCA) and for clustering analysis. Unsupervised hierarchical clustering was performed using the list of differentially expressed entities (i.e., metabolites) and conditions (resistance versus sensitivity) and Euclidean correlation and Ward's linkage rule were used as measure of similarity. Metabolite identification was performed using MPP and Fihen Metabolomics retention time locking (RTL) library (Agilent) as a reference.

2.16 Seahorse XFe96 metabolic assays

The Agilent Seahorse XF platform is an assay for assessing both mitochondrial and glycolytic function by directly measuring OCR (Oxygen Consumption Rate) and ECAR (Extracellular Acidification Rate) in real-time in living cells. The assay uses injection ports to sequentially add modulators of respiration and glycolysis into the cell culture medium in order to evaluate key metabolic parameters such as basal and maximal respiration, basal and compensatory glycolysis.

1.5–2 × 10^4 cells were seeded in XFe96 cell culture plates in 80 µL (5-8 technical replicates) and incubated at 37°C for the time required by the experimental conditions. The day of the assay, medium was replaced with 180 µL XF base medium supplemented with 10 or 25 mM glucose (10 for cells in RPMI, 25 for cells in DMEM, Sigma), 2 mM glutamine, and 1 mM sodium pyruvate (Sigma). Cells were incubated for 1 h at 37°C in a non-CO2 incubator to allow to pre-equilibrate with the XF base medium before the analysis and then subjected to the extracellular flux (XF) Glycolytic Rate Assay and/or to the XF Mito Stress Test.

2.16.1 Cell Mito Stress Test

Mito Stress Test analysis reveals basal respiration, maximal respiration, and other key mitochondrial parameters (e.g., ATP production, proton leak, non-mitochondrial oxygen consumption) by directly measuring OCR and ECAR, evaluating the ability of the cells to exploit the mitochondrial oxidative metabolism. This analysis is performed in real-time after a sequence of compounds that interfere with ETC (**Figure 16**): oligomycin (1 µM) that inhibits ATP synthase (complex V) thus decreasing the electron flow through the ETC and resulting in a reduction of the respiration function; carbonyl cyanide-4 (trifluoromethoxy) phenylhydrazone (FCCP) (1 µM), an uncoupling agent that breakdowns the proton gradient and disturbs the mitochondrial membrane potential thus the ETC is uninhibited and OCR reaches the maximum; finally a mix of Rotenone/Antimycin A (Rot/AA, 0.5 µM) that inhibits mitochondrial complex I and III, respectively, shutting down the mitochondrial respiration. Protein quantification was used to normalize the results. Basal respiration is calculated as last rate OCR measurement before injection – non-mitochondrial respiration rate. Maximal respiration is calculated as the maximum rate measurement after FCCP injection – non-mitochondrial oxygen consumption.

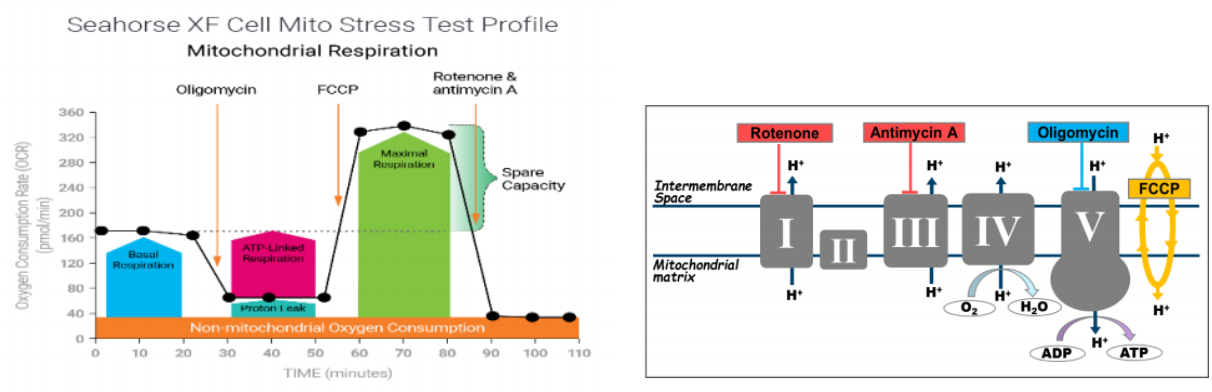

Figure 16. Agilent Seahorse XF Cell Mito Stress Test profile (left) and ETC modulators (right).

2.16.2 Glycolytic Rate Assay

Glycolytic rate assay is an accurate method for evaluating glycolysis by directly measuring OCR and ECAR in real-time, evaluating the ability of the cells to exploit the glycolytic catabolism. This test uses ECAR measurement to assess basal glycolysis and compensatory glycolysis following mitochondrial inhibition (**Figure 17**). By also concomitantly measuring OCR, the Glycolytic Rate Test discriminates the contribution of mitochondrial derived CO_2 to extracellular acidification from that of glycolysis hence subtracting the CO_2 contributing acidification from the total Proton Efflux Rate (PER) and calculating the resulting glycoPER, that is the rate of protons extruded into the extracellular medium and derived from glycolysis. The first injection is a mix of Rot/AA (0.5 μM) that inhibits the mitochondrial respiration and therefore impairs CO_2 derived protons. The second injection is 2-DG (50 mM), that inhibits glycolysis and confirms that the PER produced prior to the injection is mainly related to glycolysis.

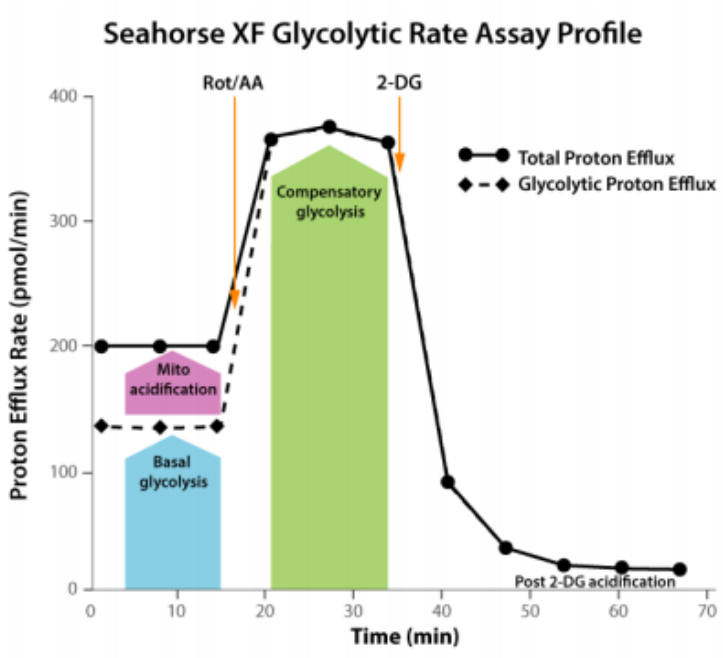

Figure 17. Agilent Seahorse XF Glycolytic Rate Assay profile.

2.17 Lung retention assay

MCF7 LTED cells transfected with anti-miR-CTR, anti-miR-23b-3p, siCTR, and siSLC1A2 were labeled with CellTracker Red CMTPX or Green CMFDA dyes (Molecular Probes), trypsinized, mixed at a 1:1 ratio, and a total of 1 million cells were injected into the tail vein of 5- to 6-week-old BALB/c mice. Mice were sacrificed at 1 and 5 h post injection, and lungs were examined with a Leica TCS SP5 microscope using x10 lens. Six images were taken for each lung. Tumor cell colonization of the lung was quantified using Fiji open platform, by converting the red and green images into separate binary images and measuring total tumor cell coverage per field of view.

2.18 Gene and microRNA expression analysis

MCF7 cells were cultured in either the recommended medium or in a medium E2 deprived for 3 days and compared to MCF7 LTED cells cultured in the standard medium. Triplicate samples from 3 independent experiments were assessed for global miRNA and gene expression by microarray analysis. Specifically, 9 samples were hybridized on Agilent whole human genome microarray (Agilent Technologies), which represents 60k unique human transcripts. The same samples were hybridized also on Agilent human miRNA microarray v16 (Agilent Technologies). One-color gene expression was performed according to the manufacturer's instructions.

2.19 Bioinformatic analysis

Microarray data were normalized and analyzed using GeneSpring GX v.14.8 software (Agilent Technologies). The probes detected in at least one sample were utilized for statistical analysis. Differentially expressed genes were selected to have a > 2-fold expression difference between groups and an adjusted P-value<0.05 at ANOVA test, with Benjamini and Hoechberg correction. Supervised hierarchical clustering was performed for OS samples with GeneSpring clustering tool using the list of differentially expressed genes and Euclidean correlation as a measure of similarity. The mRNA and miRNA anti-correlation network analyses were performed using the R software. Briefly, mRNA and miRNA found as differentially expressed in each pairwise comparison (FDR<0.05, FC<-2 or >2) were initially used to filter candidate interactors emerging from the PITA miRNA/target predictor tool. To ensure the identification of relevant interactors and limit the size of the network, the filtered collection of mRNA/miRNA pairs was further purged from experimentally validated pairs, according to the miRTarBase repository. The expression values of the remaining candidate interactors were tested for mRNA/miRNA expression anti-correlation (correlation test, Benjamini-Hochberg correction, adjusted p <0.05 and correlation

<0). The resulting networks were graphically annotated and represented using functions from the igraph R package.

2.20 Analysis of human datasets

The BRCA TCGA (The Cancer Genome Atlas) dataset analyzed is available in TCGA data portal. Gene and miRNA expression data and the corresponding clinical information for ER+ BRCA from TCGA provisional dataset were obtained through Firebrowse data portal. From the BRCA dataset, we selected samples with miRNA-mRNA and OS data. Survival analysis was performed using Kaplan-Meier curve log-rank testing, using Cutoff finder for best miR-23b-3p/SLCA6A14 and HK2 high- and low-expression selection. Information on normalization methods and multivariate analysis are available online at the KM plotter website. For HK2, the relapse-free survival (RFS) data of patients belong to the following datasets: GSE45255, GSE37946, GSE2603, GSE21653, GSE20711, GSE19615, GSE17907, GSE16391, E-MTAB-365; and the OS data of patients belong to the following datasets: GSE45255, GSE37946, GSE20711. For SLC6A14 and TNFAIP3 survival analysis, the curated dataset of ER+ breast cancers was created using Km-plotter and included the RFS data of patients belonging to the following datasets: GSE6532, GSE20711, GSE7390, GSE21653, E-MTAB-365, GSE2034, GSE2990, GSE17705, GSE12093, GSE9195, GSE3494, GSE4611, GSE45255, GSE2603, GSE16391, GSE42568, GSE26971, and GSE19615. SLC1A2 data in 52 paired ER+ breast cancer samples pre- and post-2-week letrozole treatment were retrieved using GEO (GSE5462) and normalized log2 expression values are shown either pre- or post-letrozole treatment for each patient. Correlation data on patients that have been treated with adjuvant fulvestrant were from the GSE33658 dataset. SLC1A2 and AURKA log2 normalized expression levels were reported.

2.21 Statistical analysis

Statistics were performed using GraphPad Prism 8 Software. Unless stated otherwise, all numerical data are expressed as mean ± error of the mean (SEM) and noted in figure legends. All experiments were repeated at least 3 times independently, with 3 or more technical replicates for each experimental condition. Unless stated otherwise, comparisons between 2 groups were made using the two-tailed, unpaired Student's t-test. Comparisons between multiple groups were made using one-way analysis of variance (ANOVA), and two-way ANOVA for comparisons between multiple groups with independent variables. Bonferroni and Dunnett post-testing analysis (unless otherwise stated) with a confidence interval of 95% was used for individual comparisons.

Multivariate Cox Analyses on the cohort of patients analyzed were generated using KM-plotter. Statistical significance was defined as: *, $p<0.05$; **, $p<0.01$; ***, $p<0.001$, **** $p<0.0001$, ns, not significant (or when differences were not statistically significant no indication was reported in the figures).